NBSIR 75-809

NON-PLANAR NEAR-FIELD MEASUREMENTS: SPHERICAL SCANNING

Paul F. Wac

Electromagn
Institute for
National Bu
Boulder, Co

June 1975

NBSIR 75-809

NON-PLANAR NEAR-FIELD MEASUREMENTS: SPHERICAL SCANNING

Paul F. Wacker

Electromagnetics Division
Institute for Basic Standards
National Bureau of Standards
Boulder, Colorado 80302

June 1975

U.S. DEPARTMENT OF COMMERCE, Rogers C. B. Morton, Secretary

NATIONAL BUREAU OF STANDARDS, Richard W. Roberts, Director

TABLE OF CONTENTS

TABLE OF CONTENTS (continued)

LIST OF FIGURES AND TABLES

LIST OF MATHEMATICAL SYMBOLS AND NOTATIONAL CONVENTIONS

a,b Coefficients of incoming and outgoing modes respec-
tively. Zero subscripts are used for waveguide
modes. ^ over a symbol indicates the set of spatial
modes of the given type.

$A=r_0$ Radius of the scanning sphere, i.e., the distance
between the origins of the probe and test antenna
coordinate systems. See (2) and (3).

$A^{mn}(\theta), B^{mn}(\theta)$ Auxiliary functions used in determining the
modal coefficients without probe correction. De-
fined in section 9.

$[\underline{B}_{-m''n}^{sm}]$ Backward multiplying matrix for computing the far
field.

c_M General modal coefficient. See (1).

c^{snA} An integral defined in (22').

$c_{\sigma\mu\nu}^{sn}(A)$ Probe translational transformation coefficient.
See (15) and Appendix II.

C_{2v} A symmetry group used in sections 5.1 and 8.

$d_{m\mu}^{(n)}(\theta_0)$ A factor in the representation coefficient of the
spherical point group. See (16) and Appendix I.

$D_{\underline{m\mu}}^{(n)}(R)$ A representation coefficient, the element in the
mth row and μth column of the matrix corresponding
to the operation R in the nth irreducible repre-
sentation. Used in the expression (9) for the
received signal with probe correction. See (6),
(7), and table 1.

$\underline{E}$ Electric field.

$f(P), f_M(P)$ A function (scalar, vector or tensor) of position
P, the latter function being the Mth mode.

$f_m^{(n)}(P)$ A function (scalar, vector or tensor) of position
P belonging to the mth row of the nth irreducible
representation.

$\underline{F}(R)$ A vector field or function of the scanning param-
eter R.

$[F^{m\mu}_{nm''}]$ The multiplying matrix used in computing the modal coefficients for the probe correction case (25). The elements are complex numbers. $[f^{m\mu}_{nm'}]$ and $[\delta^{m\mu}_{nm'}]$ are matrices used in the computation of $[F^{m\mu}_{nm''}]$; see (24), (25), and Appendix I.

$\underline{F}^{smn}$ A vector mode belonging to the mth row of the nth representation; for $\underline{M}$ and $\underline{N}$ modes of (6') and (6"), s is 1 and 2 respectively. $\underline{F}^{smnA}(\theta,\phi)$ is the vector value at the radius A, polar angle θ, and azimuthal angle ϕ.

$[\underline{F}^{smA}_{m''n}]$ A matrix in which the element in the m"th row of the nth column is a complex two-vector constant equal to the coefficient of $e^{im\phi}\, e^{im''\theta}$ in the Fourier expansion of $\underline{F}^{smnA}(\theta,\phi)$. Used in computing the far field after the modal coefficients (Q's) have been determined.

$g_{Mu}(\tilde{R})$ Coefficient in the expression (4) for the received signal as a function of relative positions and orientations of an antenna pair.

$G_{MU}(R)$ Corresponding coefficient in expression (5) for the received signal after transformation of the probe pattern coefficients.

$\underline{g}^{smn}_{\sigma\mu\nu}(A,\chi_0,\theta_0,\phi_0)$ $g_{Mu}(\tilde{R})$ for the spherical case (14).

$g^{(n')}_{m'}$ A function belonging to the m'th row of the n'th representation.

$\underline{G}^{smn}(\tilde{R})$ A vector function belonging to the mth row of the nth irreducible representation and with polarization s. Used to express orthogonalities between modes and to determine the modal coefficients for the no probe correction case. See (12') and (13').

$\underline{G}^{smn}(\theta,\phi)$ The vector function for the spherical case (see section 9).

$[\underline{G}^{sm}_{nm''}]$ A matrix of complex two vector constants used in determining the modal coefficients for the no probe correction case. See (25').

$[\underline{g}^{sm}_{nm'}]$	A matrix used in computing $[\underline{G}^{sm}_{nm''}]$. The element in the nth row and m'th column is the coefficient of $e^{im\phi}\, e^{im'\theta}$ in the Fourier expansion of $\underline{G}^{smn}(\theta,\phi)$. See (26').
$[\underline{g}^{sm}_{nm''}]$	A matrix used in computing $[\underline{g}^{sm}_{nm'}]$ and $[\underline{B}^{sm}_{m''n}]$. See sections 11 and 9.
g^{snA}	A constant defined in section 10.
$\underline{H}$	Magnetic field.
$\tilde{H}$	An operator used in an eigenfunction equation (see section 5.1).
k	The propagation constant $\omega(\mu\varepsilon)^{1/2}$. The x, y, z, and r components of the propagation vector are denoted by k_x, k_y, k_z, and k_r respectively.
m	Row of an irreducible representation. For the spherical case, m is the coefficient of ϕ in $e^{im\phi}$. See section 5.2.
m', m''	Coefficients of θ or θ_0 in a Fourier expansion. See (24) and (25').
M	A generic modal index for the test antenna. See (4) and page 19.
$\mathcal{M}$	A generic modal index for an antenna (1).
$\underline{M}^{(n)}_m$	A mode belonging to the mth row of the nth irreducible representation (6'). Analogous to Hansen's $\underline{M}$.
n	An irreducible representation, e.g., the spherical index n. Used as a modal index. See section 5.2 and table 1.
N_n	A constant in (6) equal to the reciprocal of the number of rows in a representation. For the spherical case, $N_n = 1/(2n+1)$.
$\underline{N}^{(n)}_m$	A mode belonging to the mth row of the nth irreducible representation. Defined in (6''). See $\underline{M}^{(n)}_m$.
O_R	A symmetry operator which acts on a function. Defined after (6).

p_u — The coefficient of mode u in the probe pattern (4), expressed in terms of the probe coordinate system. Explicitly written as $p^{\sigma\mu\nu}$ (section 5.2) or $\underset{\sim}{p}^{\sigma\mu\nu At}$ for the spherical case (17).

$p_m^{(n)}$ — Partner function belonging to the mth row of the nth irreducible representation (7).

$p^{\sigma\mu\nu At}$ — Coefficient of probe mode after translation of centers correction (15).

P — Position as in $f(P)$.

P_U — Coefficient of mode U in the probe pattern (5), after transformation of probe pattern and renormalization. Explicitly written as $P^{\sigma\mu\nu}$ or $P^{\sigma\mu\nu At}$ (section 5.2 and (16)).

$P_n^m(\cos\theta)$ — Associated Legendre function.

q_M — Coefficient of mode M in the pattern of the test antenna (4). Explicitly written as q^{smn} (section 5.2, (14)).

Q_M — Coefficient after renormalization (5). Explicitly written as Q^{smn} (section 5.2, (16)).

R — Scanning operation expressing position and orientation of probe (5). Assumed to be a symmetry group operation (section 5.1).

$\tilde{R}$ — General operation on the probe expressing its position and orientation relative to the test antenna. Assumed to be a symmetry operation in an extended group (section 5.4).

r — Radial coordinate.

$r_0 = A$ — Fixed value of the radial coordinate in spherical scanning, i.e., separation of the origins of the probe and test antenna coordinate systems.

$\mathcal{R}$ — In the scattering matrix of an antenna, the sub-matrix which represents receiving properties (3).

s — The polarization index of a mode, equal to 1 and 2 for $\underline{M}$ and $\underline{N}$ modes respectively (section 5.2).

S — In the scattering matrix of an antenna, the sub-matrix which represents the scattering properties (3).

t — An index which identifies a probe and/or its orientation.

T — In the scattering matrix of an antenna, the sub-matrix which represents the transmitting properties.

u — Generic modal index for the probe in its own coordinate system (4).

U — Generic modal index for the probe after the transformation of the probe coefficients (5).

$W^t(A, \chi_0, \theta_0, \phi_0)$ — The complex amplitude delivered to the load of the receiving antenna, normalized relative to the input to the transmitting antenna and corrected for mismatch. See after (14).

$\underline{W}^A(\theta, \phi)$ — The output W of two ideal probes, considered as a vector (16').

$\underline{w}(\theta, \phi)$ — $\underline{W}^A$ for the far field (28').

Γ — Complex reflection coefficient (3), (4) looking into the antenna. Γ_L is the reflection coefficient looking from the reference plane of the receiving antenna toward the load.

δ_{jk} — Kronecker delta, equal to unity if $j = k$, zero if $j \neq k$.

$\delta(x)$ — Dirac delta "function."

$\Delta_{m\mu}^{(n)}$ — $d_{m\mu}^{(n)}(\pi/2)$, used in computing the coefficients in the Fourier expansion of $d_{m\mu}^{(n)}(\theta_0)$. See Appendix I.

ϵ — Dielectric constant.

ϕ_0, θ_0, χ_0 — Eulerian angles expressing the position and orientation of the probe relative to the test antenna. Defined in figure 3. The azimuthal and polar angles of the probe axis are given by ϕ_0 and θ_0 respectively.

μ — Magnetic susceptibility.

μ   Row of an irreducible representation of a probe mode. See section 5.2. For the spherical case, that modal index which occurs in $e^{i\mu\phi'}$.

ν   Irreducible representation of the probe mode (section 5.2). For the spherical case, that modal index which occurs in $P_\nu^\mu(\cos\theta')$.

$[\Pi_{m'm''}]$ The matrix which corrects for integration over the polar angle from 0 to π instead of 0 to 2π in the computation of the pattern coefficients (Q's) of the test antenna (24), (26), (26').

σ   Polarization index of the probe modes (section 5.2 and (14)).

ψ   Any eigenfunction (section 5.1).

ρ(R)   A weight function in the symmetry decomposition expression (6) and the orthogonality relations (see table 1).

ω   Angular frequency.

Notational Conventions

The coordinates of the test antenna and probe coordinate systems are unprimed and (singly) primed respectively. Double and triple primes are used to indicate the transmitting and receiving antennas respectively. Single primes are used on modal indices to indicate a possibly different value. Zero subscripts are used on operations upon the probe and its coordinate system.

Script is used for symbols which do not refer to a specific antenna or symmetry group, as well as for additional symbols.

Row, column, and rectangular (or square) matrices are indicated by ⌊ ⌋, { }, and [ ] respectively. As a function is decomposed, say into its Fourier components, the variable is replaced by a superscript index. When an index is used to indicate a row or column in a matrix, it is lowered to the subscript position. When this is impractical, the index is encircled. ⌈ ⌉ is a symbol defined in Appendix II.

NON-PLANAR NEAR-FIELD MEASUREMENTS: SPHERICAL SCANNING

by

Paul F. Wacker

ABSTRACT

The advantages and limitations of near-field antenna measurements are compared with those of conventional far-field measurements. Further, the advantages and limitations of planar, circular cylindrical, and spherical scanning are compared.

Spherical scanning is advantageous for arrays steered well off-axis and for antennas with wide angle side lobes, but the data processing has been quite impractical except for very simple antennas and probes. A new highly efficient data processing scheme is given for spherical scanning with and without probe pattern correction. The translation-of-centers transformation of the probe pattern coefficients (required only with the probe pattern correction) is carried out once and for all for a given probe, scanning radius, and frequency. The routine computations involve Fast Fourier "Transforms" and multiplication by matrices with constant elements, matrices which are independent of the detailed nature of the probe, the radius of the scanning sphere, the points at which measurements are made, and the nature of the test antenna. The FFT's and matrix multiplications supplant matrix inversion, ordinary solution of simultaneous equations in more than two unknowns, ordinary numerical integration, and (in routine processing) ordinary evaluation of functions, even for computation of the far field. Except for the truncation of the infinite series of spherical modes, no analytical or data processing approximations are made, even in the use of the FFT.

So that readers may draw from their understanding of planar and cylindrical scanning, a unified theory of near-field data processing is given, treating planar, cylindrical, and spherical scanning as mere special cases.

Key Words: Antennas; arrays; coordinate transformations; data processing; group representations; measurements; near field; non-planar; patterns; scanning; spherical; symmetry.

I. QUALITATIVE DISCUSSION

1. Objectives

Determination of antenna patterns by near-field spherical
scanning is highly attractive from many points of view for
both developmental and operational testing of, e.g., airborne
arrays. It provides a small, inexpensive, all-weather antenna
range free of ground reflection effects. Unlike the planar
and circular-cylindrical scanning techniques, it is easily
applied to antennas steered well off-axis and, if the antenna
can be mounted on a conventional rotator, requires no probe
transport mechanism, as distinguished from possible rotation
of the probe about its own axis.

Although Jensen* has provided a formulation almost com-
plete in the formal sense, his data reduction scheme is
grossly impractical except for very simple test antennas.
By the use of highly-efficient data-reduction techniques
integrally related to new probe designs, it is believed pos-
sible to provide practical, efficient data reduction systems
with and without probe pattern correction, permitting realiza-
tion of the advantages of spherical scanning. The probes are
assumed to be circularly (azimuthally) symmetric in the
material sense and propagate only a single mode but are
otherwise arbitrary. However, the simpler the dependence
of the pattern upon the polar angle, the simpler the (mathe-
matical) probe correction.

The objectives of this effort are to determine the feasi-
bilities of the proposed (spherical scan) data reduction
schemes for electrically large antennas, outline the required
probe designs, and carry out the required mathematical and
numerical analysis leading to practical algorithms upon which
computer programs may be based. Further, the advantages and
disadvantages of spherical scanning compared to alternative
measurement procedures are outlined, all related to the
extent possible to antennas of interest to the Air Force.

---

*The bibliography is given at the end of this report.
References in the text are enclosed in square brackets.

2. Comparison of Techniques for Determining Antenna Patterns*

2.1 Advantages and Limitations of Near Field Scanning

The suitability of a given method of determining an antenna pattern of course depends upon the antenna. For an antenna which is both electrically and physically small, say a probe, near-field techniques seldom compete with conventional methods. However, for larger antennas, near-field techniques have distinct advantages. Ground reflections are eliminated as are the grazing-incidence reflections of "anechoic" chambers, since the test antenna and probe are close together and the absorber may be placed essentially perpendicular to the radiation. (Reflections in chambers are larger than is commonly believed; in a "good" anechoic chamber, the apparent gain may vary by 2 dB as the antenna pair is rotated with respect to the chamber.) Moreover, proximity errors do not occur, but to reduce the proximity error in a conventional measurement of a typical standard gain horn (with another horn of comparable size) to 0.05 dB requires that the measurements be made at 32 times the Rayleigh distance ($32 \ a^2/\lambda$). Further, a small, closely coupled system is subject to laboratory-type control, as compared to a conventional system with nearby trees and buildings, variable moisture content of the ground, and varying weather conditions. Hence, near field measurements can yield especially accurate antenna patterns [Kerns 1970; Newell et al. 1973; Newell and Crawford 1974; Rodgrigue et al. 1973].

A near-field system is usually much cheaper than the conventional range it replaces (assuming the availability of a computer) and requires much less expensive absorbing material than an "anechoic" chamber. From a single physical scan, the patterns for many different steering directions may be obtained for an array, or patterns for many different frequencies may be obtained for a broadband antenna. Moreover, for production line testing and adjusting of antennas, the antenna need not be moved to a conventional range between adjustments. The all-weather character of near field work is an obvious advantage, and the method may be used to determine patterns of antennas in atmospheric absorption bands, say near 60 GHz.

The limitations of near-field techniques are as follows. As the wavelength becomes quite short, determination of phase as a function of position becomes more difficult, particularly

---

*So that the reader may obtain a general understanding of the report with a minimal study of the mathematics, general material is presented in sections 2 and 3 prior to the mathematical development. Moreover, in this context, frequent reference is made to subsequent material for later detailed study.

over a large area. (Since phase is not needed for the NBS
extrapolation method, this limitation does not apply to it.)
We have obtained high accuracy with little difficulty at 60
GHz (5 mm) for antennas 100 wavelengths in diameter, but
existing systems will become inaccurate and eventually fail
in the submillimeter region. (However, a laser fringe-
counting system with servo devices can eliminate the positional
accuracy problem, even for submillimeter waves.) Further,
there are practical size limits to scanning systems. However,
large scanning systems should be less expensive (possibly
much less) than conventional terrestial ranges required for
accurate results on an antenna of a given large size. Further,
the spherical technique may be useful for physically large
antennas mounted on a rotator since probe transport is not
required; the data reduction would be expected to be manage-
able for many such antennas, particularly if no probe correc-
tion is required (see sections 5.5 and 9).

2.2 Comparison of Near-Field Scanning Techniques

Which near-field method is most appropriate also depends
upon the antenna. For a pencil beam antenna, one naturally
thinks of a transverse planar scan, not cylindrical or
spherical (unless a planar scanning system is unavailable or
impractical due to physical size). (Unless otherwise indi-
cated, planar scanning is used to mean rectangular planar
scanning and cylindrical scanning to mean circular cylindrical
scanning.) For a fan beam antenna, one naturally thinks in
terms of a cylindrical or possibly a spherical scan. For an
antenna with lobes at many angles or an array which is steered
to many different directions, both planar and cylindrical
methods become awkward but a spherical scan seems natural.

A number of factors are involved. In mechanical terms,
the "spherical scan" is the most convenient for an antenna
which can be mounted on a conventional antenna mount, simpler
than a planar or cylindrical scan since no probe transport is
needed. If the antenna cannot be tipped, azimuthal rotation
combined with probe motion on a semicircle may be used. The
lack of probe transport is important for inexpensive imple-
mentation and/or physically-large mechanically-steerable
antennas. However, in terms of data processing, the planar
scan is simplest, particularly if a probe correction is
needed.

For planar and cylindrical scans, there should ordinarily
be little radiation in any direction nearly parallel to the
plane or axis of the cylinder. Two principles are involved.
First, a very large fraction of the energy from the test

antenna should pass through that portion of the "scanning surface" over which measurements are actually made. Hence, this requires very large measurement surfaces if the radiation has a direction nearly parallel to the plane or axis of the cylinder.

(In principle, actual measurements could be extrapolated to other parts of the scanning surface, but this must be regarded as a makeshift. A directional probe could be used to decrease the required scanning area if information is required only for a restricted set of directions; if there is much radiation in directions of no interest, such a probe also improves the "signal" to "noise" ratio. (Because directional probes tend to be large, they tend to introduce multiple reflection problems, which may require special design and/or increased probe-antenna separation.) Such measurements could be made on a series of canted planes, each plane providing information for a restricted set of solid angles. Note that the planes cannot be truncated at their intersections, as in a prism. Although the measurements on such a prism would be sufficient in the abstract sense, the available data processing algorithms require that information be available as far out as there is significant contribution to the Fourier transform for angles of interest.)

Second, measurements on a surface nearly parallel to a direction of propagation are very wasteful in terms of measurement accuracy, much like measuring the cosine rather than the sine to determine a small angle; moreover, the phase changes rapidly but must be known everywhere on the measurement surface to a small fraction of 2π relative to a single reference.

An additional factor in the choice of a near-field scanning method relates to the implied choice of basis functions. Thus, for a rectangular horn, a planar rectangular scan should be efficient, while for an antenna with circular symmetry, spherical or circular cylindrical scanning makes full use of the azimuthal dependence in the choice of basis functions. A well-chosen set of basis functions for a given problem means fewer unknowns to determine and so more effective use of measurements, either through wider spacing of measurements or, for a given spacing, greater redundancy providing better statistical averaging. However, if the antenna or array is steered to many directions, the advantage of a specific set of basis functions is reduced or eliminated. Nevertheless, a spherical surface does have advantage in this situation.

3.   Spherical Scanning

3.1   Problems

Jensen has given a treatment of spherical scanning,
essentially complete in the formal sense. (He did not treat
reduction of polarization measurements.) However, his proposal
for analyzing the data was quite impractical except for quite
simple probes and test antennas. Specifically he proposed
inverting the matrix to solve the simultaneous equations re-
presented by equation (14) of this report. Even for a sphere
of only 20 wavelengths in diameter and four measurement points
per square wavelength, this would be a real matrix of order
$n = 20,000$. Assuming a fast computer, a highly efficient com-
puter program designed for large matrices, and very large
storage, inversion would require roughly $20 n^3$ microseconds,
since the matrix has few zeros. Hence, for the case cited,
the computer would run continuously for more than five years
(assuming sufficient core storage, $4 \cdot 10^8$ words for the input
matrix alone). Further, the inverse would be highly inaccurate
due to accumulated rounding error. Moreover, he proposed
numerical computation of the complicated elements of the
matrix to be inverted.

3.2   Solutions

In our procedure, presented in London in July 1974, the
simultaneous equations are decoupled into sets of at most two
equations in two unknowns (two probe orientations and two coef-
ficients for polarization-pair modes), which are easily solved.
The decoupling is achieved by means of a Fast Fourier "Trans-
form," followed by matrix multiplication. The multiplying
matrix is independent of the test antenna, the detailed nature
of the probe, the radius of the measurement sphere, the fre-
quency, and the points at which the measurements are made,
and hence may be computed once and for all. Further, it has
many conveniently located zeros.

Moreover, the FFT and matrix multiplication replace both
ordinary numerical integration and computation of both the modes
and D's of (16) as functions of ϕ, θ, ϕ_0, θ_0, and χ_0. Further-
more, the translated probe coefficients (p's of (15)) are re-
quired only with probe pattern correction and then computed
only once for each probe and scanning radius, independent of
the test antenna and the points at which measurements are made.

Both the translational transformation and the decoupling are markedly simplified by the choice of probes which have simple azimuthal dependence (μ of (14) to (18) equal to 0 or $\pm$ 1). Moreover, since the patterns of these probes have precisely the same azimuthal dependence as those of ideal dipoles, they are expected to reduce the need for a probe pattern correction. These probes should have circular symmetry in the physical sense and the leads, e.g., waveguide, should transmit only a single mode, but the probes may have arbitrary flare. The modal coefficients expressing the pattern of the test antenna so computed are least squares values, and tests of statistical significance (see section 10) are easily applied, permitting discrimination against random error and reduction in subsequent computations. The far field is computed from the coefficients by an inverse FFT following multiplication by a matrix closely related to the aforementioned multiplying matrix. It also may be computed once and for all by techniques similar to those for the other matrix, no inversion being required. Some of these ideas are expressed in a paper recently submitted by Jensen, but not θ_0 decoupling by matrix multiplication, avoidance of computing the θ_0 dependent functions, or efficient computation of the far field by an FFT and matrix multiplication.

3.3 Limitations of the New Spherical Scanning Technique

As previously indicated, the mechanical limitations of the spherical scan method are very slight for an antenna mounted on a rotator. The Fast Fourier "Transform" for the spherical case is little more complicated than for the planar case and the matrix multiplication is fast, particularly due to the many conveniently located zeros in the matrix. Hence, in terms of scanned area measured in square wavelengths, these operations may be little more restrictive for the spherical than the planar case. Further, the limitations arising from computing the multiplying matrix and the translational transformation of the probe pattern are moderated by the fact that they may be computed once and for all (the latter for a given probe and scanning radius). Moreover, the translational transformation may be eliminated if the probe may be approximated as an ideal dipole (see sections 5.5 and 9), and computation of the multiplying matrices is feasible if the reactive zone of the antenna may be circumscribed by a sphere with no more than 250 half wavelengths on a great circle (see section 8 and Appendix I). However, as for cylindrical scanning, the complexity of the transformational transformation of the probe pattern creates computational problems for large near-field scanning radii with complicated probe patterns. The transformation is simplified by the fact that $c_{\sigma\mu\nu}^{sn}$(A)'s of equation (15) are needed only for

6

$\mu = 0$ or ± 1 and the fact that these quantities are simpler for these cases, relatively simple explicit expressions and two-term recursion relations being available for the coefficients of the Hankel functions for both the $\mu = 0$ and ± 1 cases. The coefficients of the Hankel functions may be computed once and for all, independent of the specific probe or the diameter of the scanning sphere. The upper limit on the diameter with the probe correction remains to be determined, but it is believed that the correction will be feasible for most of the radii for which it is needed.

II. GENERAL MATHEMATICAL BACKGROUND

4. General Theory of Antennas and Antenna-Antenna Interactions

Due to the mathematical complexity of the spherical problem, some basic discussion is given to facilitate understanding. So that the spherical problem may be related to simpler problems, the discussion is initially in general terms. This presentation is independent of the coordinate system and applies, e.g., to planar, circular cylindrical, and spherical scanning as special cases. Although attention is fastened upon electromagnetic fields, the treatment applies equally well to acoustic fields in mathematically linear fluids, without the complication of polarization. So that readers familiar with planar and/or circular cylindrical scanning may transfer their understanding to the spherical case, examples from these types of scanning are given. However, these examples may be disregarded by those not familiar with them.

The general treatment constitutes a summary of pertinent parts of forthcoming papers. Although section 5 is based upon the theory of group representations, no familiarity with the theory is required, provided that the reader accepts (6), (7), (10) to (12), (12'), and (12"), which are related to familiar examples. Although the theory may seem needlessly general, most of the equations presented and explained are needed for the spherical case, but apply (without specific functional forms) to any compact group, essentially to any smooth finite scanning surface. The remaining equations are the counterparts for the planar and cylindrical cases. Readers finding difficulty with Part II may skim it for the basic ideas and then refer to it while reading Part III on spherical scanning proper.

Any field $f(P)$ may be approximated in the mean to any desired accuracy as a linear combination of any complete set of suitable basis functions $f_M(P)$, say a complete set of exact solutions of Maxwell's equations for which we use the word mode. Thus

$$f(P) = \sum_M c_M \, f_M(P), \qquad (1)$$

where P indicates position. (A single frequency and hysteresis free media are assumed.) The modes may be, e.g., waveguide modes, plane waves of specified direction and polarization, circular-cylindrical modes, or spherical modes.

Usually one uses spatial modes which are solutions for media surrounding an antenna or scatterer. In this case, the domain of validity of eq. (1) (with constant coefficients) is limited; for example, a series of ordinary spherical modes representing the field outside a sphere circumscribing a transmitting antenna does not represent the field inside, particularly for a reëntrant body; the modes are not solutions of Maxwell's equations for the whole domain.

The modal index M implies a complete identification of a mode including the polarization (e.g., TE, TM character). (Script letters are used in abstract treatments, e.g., a single isolated antenna or symmetry not pertaining to a given antenna or coordinate system, as in (1), (3), (6), and (7).) Kerns and Dayhoff use m, k_x, and k_y or n, ℓ_x, and ℓ_y for the planar case. Leach and Paris use n and h (or η), as well as the distinction between a and b or between c and d to indicate the TE, TM character. Jensen uses s, m, and n (or σ, μ, and ν) for the spherical problem. Note that k_x, k_y, ℓ_x, ℓ_y, h and η assume continuous values. (See section 5 and table 1 for details.) In these cases, the summation signs in eqs. (1), (2), (4), and (5) are symbolic and really imply integration. Similarly, the matrices in (3), (4), and (5) and in Kerns and Dayhoff are symbolic. Hence, in the abstract mathematics, as distinguished from practical data processing, the matrices have infinite order and may have either a denumerable or non-denumerable number of rows and columns.

Assuming that the materials (medium and material(s) in the antenna and waveguide) are mathematically linear, the coefficients c_M of the basis functions (modal expressions) f_M for a source-free domain are related by a scattering matrix, just as for a waveguide junction. That is, in a region free of sources, the coefficients of the outgoing waves {b} are given by linear combinations of the coefficients of the incoming waves {a}, i.e., by the matrix equation {b} = [S]{a}, or

$$b_i = \sum_j S_{ij} a_j. \tag{2}$$

The S's are complex functions of frequency or, for a single frequency, complex constants [Kerns and Beatty, p. 41 ff.].

For simplicity for an antenna or array, only one non-zero waveguide output mode coefficient b_0 and only one non-zero waveguide input mode coefficient a_0 are assumed, and the remaining output and input coefficients (of the spatial modes)

9

are designated by $\hat{b}$ and $\hat{a}$. Then, the matrix equation may be partitioned to yield

$$\left\{ \begin{matrix} b_0 \\ \hline \hat{b} \end{matrix} \right\} = \left[\begin{array}{c|c} \Gamma & R \\ \hline T & S \end{array} \right] \left\{ \begin{matrix} a_0 \\ \hline \hat{a} \end{matrix} \right\} , \tag{3}$$

where Γ is the input reflection coefficient of the antenna, and T, R, and S represent all its transmitting, receiving and scattering properties. See figure 1. (Note that Γ is a complex number and that R and T consist of a single row and column respectively of such numbers.) Kerns and Dayhoff designate these as S_{00}, S_{10}, S_{01}, and S_{11}, respectively. Leach and Paris use $a_n(h)$, $b_n(h)$ and $c_n(\eta)$, $d_n(\eta)$ to express T for the test antenna and probe respectively, while Jensen uses q^{smn} and $p^{\sigma\mu\nu}$ respectively.

For an antenna pair, neglecting multiple reflections between the antennas, the ratio of b_0 for the receiving antenna to a_0 for the transmitting antenna is given by a bilinear form between the T for transmitting antenna and the R for the receiving antenna, due to the assumed linearity. That is, the ratio is given by a weighted sum of products between the T's and the R's, where the weights depend upon the relative coordinates and orientations of the two antennas. See figure 2. Since we are interested in the pattern of the test antenna in its own coordinate system, we consider the test antenna to be fixed and the probe to be moving; happily, we need not distinguish whether the test antenna transmits to the probe or vice versa, since the T's and R's (as distinguished from the Γ's of the mismatch correction) occur in a symmetric manner in the bilinear form.

Consider a pair of coordinate systems, namely an unprimed system fixed to the test antenna and a (singly) primed system fixed to the probe. Let the T's or R's (transmitting or receiving pattern) of the test antenna be represented by the row matrix $\lfloor q_M \rfloor$ and those of the probe (receiving or transmitting pattern) by the column matrix $\{p_u\}$, the elements in each matrix referred to modes fixed in the coordinate system of the given antenna, where M and u are modal indices. (For quantities characteristic of the original independent coordinate systems, lower case is used, except for M and the transformation operator $\tilde{R}$, as in (4).) Assume that the test antenna is fixed in space and that the probe moves on a scanning surface and let $\tilde{R}$ be a set of translation(s) and/or rotation(s) which transform the fixed (test antenna)

coordinate system into the moving (probe) coordinate system. The $\tilde{R}$'s thus serve as position coordinates and orientation parameters for the probe relative to the test antenna. Then the complex amplitude delivered to the load of the receiving antenna is given by

$$b_0''' (\tilde{R}) = \frac{1}{1-\Gamma''' \Gamma_L'''} \sum_M \sum_u q_M \, g_{Mu}(\tilde{R}) \, p_u \, a_0''$$

$$= \frac{1}{1-\Gamma''' \Gamma_L'''} \lfloor q_M \rfloor \, [g_{Mu}(\tilde{R})] \, \{p_u\} \, a_0''. \tag{4}$$

Double and triple primes are used for the transmitting and receiving antennas respectively. The coefficient of the sum is a mismatch correction, Γ_L''' and Γ''' being the complex reflection coefficients at the reference plane of the receiving antenna looking toward the load and antenna respectively (with the antenna in free space) [Kerns 1971, (1.6-11)(1.6-15)]. (Jensen, Leach and Paris, and Kerns and Dayhoff do not include the mismatch correction, and the first two papers assume that the probe receives.) Except for the functional character of the g's (as yet unknown), (4) follows from the linearity and lack of multiple reflections. Validity upon close approach of the antenna pair depends upon the individual coordinate system(s).

Normally one position coordinate is held fixed (z_0 coordinate in the planar case and the radius r_0 in the cylindrical and spherical cases) and the other two varied. Further, the axis of the probe is normally kept perpendicular to the scanning surface, as in the planar, cylindrical, and spherical cases, fixing two orientation parameters. Moreover, except for rotation to determine polarization effects, the third orientation parameter is also fixed. Using zero subscripts for the $\tilde{R}$'s (in conformity with Jensen and with Leach and Paris) and enclosing the coordinates held fixed on a scanning surface in parentheses, the R's for the planar, circular cylindrical, and spherical cases are respectively x_0, y_0, (z_0), ϕ_0, z_0, (r_0), and ϕ_0, θ_0, χ_0, (r_0). The Eulerian angles ϕ_0, θ_0, and χ_0 are defined by figure 3. R without overlining is used to indicate those parameters of $\tilde{R}$ which change during scanning. Note that only R, the b_0''''s, and the g's vary during scanning. Further, note that the modes used to express the probe pattern may be different from the modes used to express the pattern of the test antenna. If correction is made for the probe pattern, it is convenient to use modes which are the same except for translation and/or rotation.

However, if no probe correction is made, dipole modes, based upon a spherical coordinate decomposition, are used for the probe, regardless of the modes used for the test antenna.

Particularly for cylindrical and spherical scanning, it is convenient to break up the determination of the g's, i.e., transformation of the probe coefficients, into two parts, the first related to the shift in the coordinate held constant during the scanning and the second related to the parameters R changed during scanning. The first may be carried out once and for all for a given probe, frequency, and scanning surface, significantly reducing data processing time. After the first transformation, (4) becomes

$$
\begin{aligned}
b_0''{}'(R) &= \frac{1}{1-\Gamma'''\Gamma_L'''} \lfloor Q_M \rfloor \, [G_{MU}(R)] \, \{P_U\} \, a_0'' \\
&= \frac{1}{1-\Gamma'''\Gamma_L'''} \sum_M \sum_U Q_M \, G_{MU}(R) \, P_U \, a_0'',
\end{aligned}
\tag{5}
$$

where the probe coefficients are corrected for the difference in the constant scanning parameter (e.g., z_0 in the planar case and r_0 in the cylindrical and spherical cases). Note that the indices of the probe modes are in general changed; see Section 5.4. Capital letters are now used for the pattern coefficients of both the test antenna and probe, since it may be convenient to renormalize both sets of coefficients, at least so that the $G_{MU}(R)$'s are unity for R = 0, i.e., for the probe pattern expressed in terms of the coordinate system of the test antenna. Capital letters are generally used for this shifted coordinate system.

Equations (1) to (5), like the remainder of this report but unlike the work of Jensen and of Leach and Paris, apply to non-reciprocal antennas, such as arrays with ferrite phase shifters; unlike their work, the receiving pattern of the receiving antenna is used, not its transmitting pattern. These equations also apply for lossy, inhomogeneous, anisotropic media, such as the atmosphere near 60 GHz or high altitude plasmas.

5. Unified Theory of Near Field Data Reduction

Reduction of the near field antenna measurements consists primarily in determining the Q_M's of the test antenna from the measured $b_0''{}'(R)$'s and the previously determined P's of the

12

probe. In principle, one can solve the simultaneous equations implied by (4) by matrix inversion as Jensen proposes, but this is highly inefficient. Since there are commonly thousands of simultaneous equations, efficient data reduction is essential and requires decoupling of the simultaneous equations (5) based upon the properties of the $G_{MU}(R)$'s, preferably using orthogonalities with respect to summation on the measurement lattice and using the Fast Fourier "Transform."

Very generally, these efficient data reduction techniques are provided by the powerful theory of group representations (mathematical theory of symmetry) referred to the scanning surface. In fact, this theory provides the appropriate modes, modal indices, G's, orthonormalities between the modes and between the G's leading to efficient data reduction, and even the g's (correction of probe pattern for the shift of the coordinate held constant during scanning).

Those not familiar with group representations may find it useful to read Chapter 3 and pages 311-317 of Hamermesh; although the chapter deals only with groups containing a finite number of operations, the basic symmetry equations of this report ((6), (7), and (10) to (12)) are closely related to similar equations there.

The following treatment has wide applicability in the abstract, but definition of the limits of applicability is inappropriate here. The surfaces are assumed smooth and of finite area, except for the plane, circular cylindrical, and other specifically mentioned cases (see comments after (12).) The representation coefficients (D's) are known only for a limited number of surfaces, commonly only after addition theorems for the functions involved are known.

5.1 Modal Symmetries

The situation is summarized in table 1, which gives correspondences which relate planar, circular cylindrical, and spherical scanning to each other and to the Fourier transform and Fourier series decomposition (real line and circle respectively). Frequent reference to the table will provide many concrete examples for the following general theory, as will reference to Part III on spherical scanning.

Just as any function of x may be uniquely decomposed into two functions, one even and the other odd with respect to reflection in the x = 0 plane, so any field (scalar, vector, or tensor) or function f of position P, may be uniquely decomposed by means of eq. (6) [Haig et al.,

Chapter 5] into a set of functions $f_m^{(n)}(P)$, each with pre-
scribed properties with respect to the operations R, which
are now assumed to form a mathematical group. Thus,

$$f_m^{(n)}(P) = N_n \int_R D_{mm}^{(n)}(R)^* \, \rho(R) \, O_R f(P) \, dR. \qquad (6)$$

This may be proved in a manner analogous to Hamermesh's (3-189);
see Haig et al. [their Chapter IV] for additional background.
The operator O_R translates and/or rotates the function $f(P)$
from the fixed (test antenna) coordinate system into the
moving (probe) coordinate system, that is, if R moves point
P to point P', then $O_R f(P)$ has the same value at P' as $f(P)$
had at P. In other words, referred to the probe coordinate
system, $O_R f(P)$ is an unchanging function [Hamermesh, pp.
80-81]. N_n is a normalization constant to be defined, $\rho(R)$
is a prescribed weight function, and the asterisk indicates
the complex conjugate. The operator O_R acts on the complete
function, e.g., for a vector function or field, it acts simul-
taneously upon the unit vectors and their functional coeffi-
cients [Kerns, 1951]. Each representation consists of a
set of matrices, one for each R; $D_{m\mu}^{(n)}(R)$ is the element in
the mth row and μth column of the matrix corresponding to
the operation R in the nth representation.

For simplicity, we confine ourselves to irreducible
unitary representations, i.e., representations consisting of
unitary matrices such that the matrices of a representation
cannot be simultaneously reduced by a unitary transformation,
that is, the representation decomposed into two or more
representations, each consisting of matrices of lower order
[Hamermesh, p. 92-98]. The irreducible unitary representa-
tions are determined only up to a unitary transformation.
For example, $e^{in\phi}$, $e^{-in\phi}$, cos $n\phi$, and sin $n\phi$ all belong to
the nth irreducible representation of $C_{\infty \, v}$, the group which
includes reflection as well as rotation on a circle, the
first two functions belong to separate rows in one formula-
tion, the last two to separate rows in another formulation.
In general, a complete orthogonal set of functions belonging
to a given representation defines that representation in
detail and each such function belongs to a specific row
[Wigner, pp. 110-111]. The number of such functions is
equal to the order of the matrices, one for the planar and
cylindrical cases, and 2n+1 for the spherical case . We are
primarily concerned not with a small number of operations R,
but a non-denumerable number, leading to an infinite number
of representations and of well-defined symmetry types $f_m^{(n)}(P)$.

For the scalar case, there is only one function with each symmetry and a set of such functions is complete and linearly independent [Pontrjagin, pp. 116-125]. Thus, for a function on a circle, there can be rotation by any real angle ϕ_0, and the Fourier series decomposition $f(\phi) = \sum\limits_{n=-\infty}^{\infty} c_n e^{-in\phi}$ is just a symmetry decomposition [Hamermesh, pp. 322-5]. Similarly, for a function on the x axis, there can be any real translation x_0, and the Fourier transform $f(x) = \int\limits_{k_x=-\infty}^{\infty} g(k_x) e^{-ik_x x} dk_x$ is a symmetry decomposition [Hamermesh, pp. 486-489]. On the surface of a sphere, the Eulerian angles (rotations) ϕ_0, θ_0, and χ_o can assume any real values, leading to the symmetry decomposition $f(\phi,\theta) = \sum\limits_{n=0}^{\infty} \sum\limits_{m=-n}^{n} c_{nm} e^{im\phi} P_n^m(\cos \theta)$ [Hamermesh, pp. 325-337; Edmonds, Chap. 4]. Even the functions e^{ix}, cos x, sin x, Bessel functions, and the associated Legendre functions may be defined on the basis of symmetry. The theory of group representations not only defines these and similar decompositions but also provides orthogonalities (12') which are used in computing the series coefficients and are basic to the definitions of the transforms.

Returning to the general case (from the scalar case), a function of a given symmetry type is denoted by $f_m^{(n)}$ and is said to belong to the mth row of the nth irreducible representation, i.e., n and m are the principal and subsidiary symmetry indices and $1/N_n$ is the number of rows in the nth representation (2n+1 for the spherical case). Of the cases presented in the table, the row index m is needed only for the spherical case, there being only one row in the other cases. As shown in the table, the planar case is just a combination of two translations, while the cylindrical case is just a combination of a rotation and a translation; hence, two indices are needed to specify n in the planar and cylindrical cases. The parameters k_x, k_y, and k_z assume all real values, while n and m assume only integer values, and n is non-negative in the spherical case. The spherical functions are those of a multipole expansion, 2^n being the order of the pole (dipole, quadrupole, octapole, hexadecapole for n = 1, 2, 3, and 4); further, the TM and TE modes represent electric and magnetic multipoles respectively. Hansen's spherical wave functions [Stratton, p. 416] have these properties, but we use slightly different definitions (see table 1 and section 6). For those familiar with quantum mechanics, the spherical n and m are $2\pi/h$ times

the total angular momentum J and its z component J_z respectively. Scalar functions belonging to the given symmetry types are given in table 1.

For the electromagnetic case, we assume for simplicity in presentation that the medium is homogeneous, isotropic, and source free. Then every solution of Maxwell's equations obeys the eigenvalue equation

$$\nabla \times \nabla \times \underline{E} = k^2 \underline{E} \text{ or } \nabla \times \nabla \times \underline{H} = k^2 \underline{H}$$

where E and H are the electric and magnetic field, the eigenvalue $\overline{k}^2 = \omega^2 \mu\epsilon$, ω is the angular frequency, and the magnetic susceptibility μ and the dielectric constant ϵ are assumed to be scalar constants.

Now consider any eigenvalue equation $\tilde{H}\psi = k^2\psi$ and any group such that every group operation R commutes with the operator H, i.e., RH = HR. Then one may choose a complete set of solutions of the eigenvalue equation such that every solution belongs to a row of an irreducible representation of the group. Moreover, the gradient, divergence, and curl each commute with any rotation, reflection, or translation [see Kerns 1951]. Therefore a complete set of solutions of the curl-curl equation -- and therefore a complete set of solutions of Maxwell's equations -- may be chosen such that every solution belongs to a row of an irreducible representation of any group which includes, e.g., only rotations, translations, and/or reflections. Further, these solutions will be orthogonal in the sense of section 5.5. This principle yields the $e^{-ik_z z}$ z dependence for waveguide of arbitrary cross-section, the curl-curl operator commuting with z translation (see table 1).

We choose our solutions to belong to rows of irreducible representations and hence (6) describes the behavior of the solutions with respect to the scanning operations (say two coordinates) assuming the representation coefficients (D's) to be known. It should be noted that the coordinate system is not assumed to (a) be orthogonal, (b) be one of the 11 coordinate systems formed from first and/or second degree surfaces, or (c) provide separation of either Maxwell's equations or the scalar Helmholtz equation. However, holding a coordinate constant on a scanning surface implies some separation with respect to that coordinate.

The application of (6) to vector fields requires care since the effects of rotation and reflection on the unit vectors must be considered. In general, one must distinguish between true or polar vectors and pseudo or axial vectors

[Stratton, p. 67]. Upon reflection the former behave like the associated arrow, while the latter behave like a directed loop normal to the usual arrow [Kerns, 1951]. Thus, in the conventional representation of a magnetic field by axial vectors, the field reflects like the associated current loops.

For simplicity in treating vector fields, we confine ourselves to an artifice which suffices in many cases. We introduce the product of a scalar function $f_m^{(n)}$ belonging to a row of an irreducible representation with a vector field $\underline{e}_i \delta$ which is invariant under all operations of the group. Since reflection is not a possible scanning operation, we need not distinguish between polar and axial vectors even in taking the curl, which converts axial to polar and vice versa. The invariant vector field is commonly taken to be the unit vector $\underline{e}_z$ in the z direction for planar and cylindrical scanning, but need not be. For example, for plane polar scanning or circular scanning $\underline{e}_z$, $\underline{e}_\phi$, $\underline{e}_r$, and every linear combination of them are invariant under the scanning operations.

Then the function $\underline{e}_i \, f_m^{(n)} \, \delta$ belongs to the mth row of the nth irreducible representation, where f and δ are scalar functions of those coordinates which are variable and constant respectively during the scanning. (The function δ may be determined by whether the mode is incoming or outgoing and either from the reduced (usually one dimensional) differential equation or equivalently by symmetry with respect to a larger group (see section 5.4 and table 1).) In analogy with Hansen's treatment [Stratton, Chapter VII], we introduce the functions

$$\underline{M}_m^{(n)} \equiv \nabla \times (\underline{e}_i \, f_m^{(n)} \, \delta) \qquad (6')$$

$$\underline{N}_m^{(n)} \equiv (1/\omega) \, \nabla \times \underline{M}_m^{(n)} \qquad (6'')$$

We write $\underline{F}^{smn}$ to indicate either $\underline{M}_m^{(n)}$ or $\underline{N}_m^{(n)}$, using s equal to 1 or 2 to indicate $\underline{M}$ or $\underline{N}$ respectively. Unlike Hansen's original development, these equations provide constructive (as opposed to hit or miss) procedures for obtaining modes with natural non-constant definitions of transverse. More importantly, they satisfy (6) and particularly (7) for their variation during scanning operations, without complications due to variation of the unit vectors during scanning. (To satisfy (7) in its simple form, the f's must be normalized as described after (7).) From their construction, the $\underline{M}$'s and $\underline{N}$'s are linearly independent and remain so during scanning.

The $\underline{M}$'s and $\underline{N}$'s actually obtained by the preceding arti-
fice obey the divergence condition and belong to a specific
row of a specific irreducible representation as do the solu-
tions of Maxwell's equations. However, for some groups or
coordinate systems, some of the $\underline{M}$'s and $\underline{N}$'s may not exist, say
those formed with $\underline{e}_i = \underline{e}_\phi$ [Morse and Feshbach, p. 1764 ff.].

That is, for some coordinate systems, some solutions of
Maxwell's equations and some fields of given symmetry may be
inconsistent with the functional forms (particularly the
factorization) arbitrarily imposed by (6') and (6"). In
such cases, direct application of (6) may yield the missing
solutions of Maxwell's equations.

5.2   Coordinate Transformations of Modal Functions

The modes then have known symmetry properties which may
be used to determine the G's as functions of R and decouple
the equations. Just as the behavior of an even function and
of an odd function under reflection in the x = 0 plane is well
defined, so is the behavior of each function $f_m^{(n)}(P)$, $\underline{M}_m^{(n)}$,
and $\underline{N}_m^{(n)}$ under each of the symmetry operations R of the group.
Here we have a non-denumerable number of symmetry operations,
so the behavior on the whole scanning surface is prescribed.
Specifically, the following equation (7) gives a function or
mode (of a given symmetry) fixed in the probe (moving) coordi-
nate system in terms of functions or modes in the test-antenna
coordinate system fixed in space. (See after (6) for the
definition of O_R.)   Thus,

$$O_R p_\mu^{(n)}(P) = \sum_m p_m^{(n)}(P)\ D_{m\mu}^{(n)}(R). \qquad (7)$$

(For a simpler analog, see Hamermesh [p. 111 (3-66)].) The
$p_\mu^{(n)}$'s are partner functions, i.e., functions $f_\mu^{(n)}$, $\underline{M}_\mu^{(n)}$, or
$\underline{N}_\mu^{(n)}$ of a given symmetry but with relative normalizations such
that (7) is valid for all μ values of a given representation
n. Note that only functions of the same representation (n)
but various rows (m) are involved; an example is given by the
equation

$$\cos n(\phi \pm \phi_0) = \cos n\phi \cos n\phi_0 \mp \sin n\phi \sin n\phi_0,$$

$\cos n\phi$ and $\sin n\phi$ belonging to the same nth representation
but different rows of the group $C_{\infty v}$ which includes reflection

18

as well as rotation on a circle. (This group provides the basis for the sine-cosine Fourier series decomposition.) For planar and circular cylindrical scanning, the sum in eq. (7) has only a single term, there being only a single row in the representations. Equation (7) provides "addition theorems" for functions. For example, the group defined by plane polar coordinates provides definitions of the cylindrical Bessel functions and, through (7), Graf's addition theorem for Bessel functions, used by Leach and Paris for the translation of axis (r_0) correction for circular cylindrical scanning.

For mathematical simplicity in the application of eq. (7), we choose the modes to be partner functions. For the $\underline{M}$'s and $\underline{N}$'s, this is achieved by choosing the scalar $f_m^{(n)}$'s to be scalar partner functions. For the probe pattern correction case, the same modes (including the same polarization properties) are chosen for the test antenna and probe for $\check{R} = 0$ (superimposed coordinate systems), but the probe modes are fixed in the moving probe coordinate system. Each modal index includes a polarization index, row index(es), and representation index(es). They are designated as follows:

	test antenna M	probe u	U
polarization index	s	σ	$\bar{\sigma}$
row index(es)	m	μ	$\bar{\mu}$
representation index(es)	n	ν	$\bar{\nu}$

Following Jensen, Latin letters are used for the test antenna and the corresponding Greek letters for the probe, Tilde overlining is used for modes defined relative to the extended group ($\check{R}$'s), while no underlining is used for the group defined by the scanning surface (R's). The larger group is used for the transformation of probe coefficients ((4) to (5)) and is discussed in section 5.4. The reader not interested in probe pattern correction may skip to section 5.5.

We can now determine the G's of (5) as functions of R. Equation (5) states that the probe mode U of polarization $\bar{\sigma}$, row $\bar{\mu}$, representation $\bar{\nu}$ and coefficient P_U in the probe coordinate system gives rise in the test antenna system to a

mode M (among others) with polarization s, row m, representa-
tion n, and coefficient $G_{MU}(R)$ P_U. Equation (7) states that
the same probe mode U gives rise in the test antenna coordi-
nate system to a mode with polarization $\bar{\sigma}$, row m, representa-
tion $\bar{\nu}$, and coefficient $D_{m\mu}^{(\bar{\nu})}(R)$ P_U. Further the coefficient
is zero unless $n = \bar{\nu}$ due to (7) and unless $s = \bar{\sigma}$ provided
that the polarization type remains unchanged during scanning
(under the R's, see section 5.1). Moreover, the fact that
the same modes are used for the test antenna and probe for
R = 0 permits identification of the summation index of (7)
with m of M. Hence,

$$G_{MU}(R) = D_{m\mu}^{(n)}(R)\ \delta_{n\bar{\nu}}\ \delta_{s\bar{\sigma}} \qquad (8)$$

where $\delta_{nN} = 1$ if n = N but zero if n $\neq$ N. Thus, (5) becomes

$$b_0^{''\,'}(R) = \frac{1}{1-\Gamma^{''\,'}\Gamma_L^{''\,'}} \sum_{smn\bar{\mu}} Q^{smn}\ D_{m\mu}^{(n)}(R)\ P^{s\bar{\mu}n}\ a_0^{''} \qquad (9)$$

which expresses the variation of the received signal on the
scanning surface. The modal indices M and U are expressed
explicitly, i.e., we write Q^{smn} for Q_M and $P^{s\bar{\mu}n}$ for P_U,
making use of the δ functions of (8) in the latter case.
Note that no term contributes to eq. (9) unless the modes of
the test antenna and probe, each in its own (translated)
coordinate system, belong to the same representation and have
the same polarization.

5.3 Orthogonalities and Decoupling the Equations

To decouple the equations, orthogonalities are required.
These are provided by the equations [Pontrjagin, pp. 110-116]

$$\int_R D_{m\mu}^{(n)}(R)\ D_{m'\mu'}^{(n')}(R)^*\ \rho(R)\ dR = \delta(k_x-k_x')\ \delta(k_y-k_y') \qquad (10)$$

$$= \delta_{nn'}\ \delta(k_z-k_z') \qquad (11)$$

$$= \delta_{nn'}\ \delta_{mm'}\ \delta_{\mu\mu'}/N_n, \qquad (12)$$

where (10), (11), and (12) apply respectively to the planar,
circular cylindrical, and spherical cases, and $\delta(x)$ is the
Dirac delta "function." Primes on modal indices merely indi-
cate distinct index values, not a coordinate system or an

antenna. Equation (12) applies to any "compact" group, essentially to any smooth coordinate surface of finite area (but not to a plane or cylinder), and (10) and (11) are analogs of (12) for two non-compact cases. The preceding equations of this section 5 apply for any compact group and the cases given, but extension to other cases requires individual investigation. (The general theory of representations of non-compact groups is not well understood except for two classes and not simple for these two [Haig et al., p. 295 ff]. Even for compact groups, each irreducible representation here consists of a non-denumerable number of matrices, one for each R, the row and column being indicated by the first and second subscripts on the D's; further, there is an infinite number of irreducible representations. However, for the planar case, there is a non-denumerable number of irreducible representations and, for the plane polar coordinate case, the matrices forming the irreducible representations are of infinite order.)

Because of eqs. (10) to (12), multiplication of both sides of eq. (9) by $D_{m'\mu'}^{(n')}(R)^* \rho(R)$ and integrating over R (all values of the scanning parameters on the scanning surface) yields

$$\int_R b_0^{'''}(R) \; D_{m'\mu'}^{(n')}(R)^* \; \rho(R) \; dR = \frac{1}{1-\Gamma^{'''}\Gamma_L^{'''}} \sum_M{}' \sum_U{}' \; Q_M \; P_U \; a_0^{''}, \quad (13)$$

where the "double" sum now contains only two terms, one for each polarization, both the row and the representation of both the probe and test antenna modes being specified. Unless a single polarization can be assumed, measurements are made with two probes or one probe with two orientations, so that eq. (13) decouples the simultaneous equations (9) into sets of two equations (probe orientations) in two unknowns (coefficients for the two polarizations). Note that no assumptions or approximations have been made concerning the polarization of either the near field (as a function of position) or the far field (as a function of direction) of either the test antenna or probe(s) except that the two by two matrices of the probe coefficients be non-singular.

The preceding analysis together with table 1 explains why decoupling of the simultaneous equations is obtained by the Fourier transform in the planar case, the Fourier transform-Fourier series decomposition in the circular cylindrical case, and by the representation coefficients of the spherical point group in the spherical case.

5.4 Probe Pattern Transformation

The addition theorem expression (7) is also useful in obtaining the probe pattern coefficients of (5) from those of (4), i.e., in transforming the probe coefficients to those characteristic of a zero value of the coordinate held fixed in scanning (z_0 for the planar case and r_0 for the cylindrical and spherical cases). Consider the group of operations $\tilde{R}$ which includes both the scanning parameters R and those held fixed during scanning, then (7) is valid with R replaced by $\tilde{R}$ and the D's of the scanning group replaced by those of the larger group. The modified (7) is then used to obtain the g's of (4). For the planar case, this just adds the factor $e^{+ik_z z_0}$ to $D_{m\mu}^{(n)}(R)$, i.e., the correction factor for the probe pattern coefficients is just $e^{+ik_z z_0}$. For the cylindrical case, this gives Graf's addition theorem for Hankel functions, used by Leach and Paris for this transformation. Moreover, for these two cases, change of z_0 or r_0 does not change TE to TM modes or vice versa, TE and TM being defined relative to a z_0 = constant plane. Hence, the probe pattern transformations are simply obtained with eq. (7).

For the spherical case, translation of the center of the probe coordinate system from r_0 = 0 to r_0 = r_0 mixes TE and TM modes, these modes being transverse with respect to surfaces of concentric spheres. Hence, Jensen's $C_{\sigma\mu\nu}^{sn}(A)$'s are non-zero even for s ≠ σ if μ ≠ 0 (see eq. (15)). See Appendix II for details.

5.5 Data Reduction Without Probe Pattern Correction

A marked simplification of the data processing may be achieved if the probe may be treated as a (high impedance) ideal dipole which gives a field component at a point. In this case the two antenna problem disappears and with it the need for coordinate transformations of the probe modal functions, both during the scanning process (eq. (7)) and due to the coordinate held fixed during scanning (section 5.4 and (15)). The elimination of the latter transformation is particularly helpful in the spherical and cylindrical cases.

Even with probes made from conventionally sized rectangular waveguide, moderate accuracy can be obtained by treating the probe as an ideal dipole. It is of course well known that the pattern of a short dipole is very similar to

that of an ideal dipole. The probes described in section 7
as well as electric dipoles short compared to half a wave-
length should provide a significantly better approximation
than rectangular guide.

From a mathematical viewpoint, $g_{Mu}(\tilde{R}) \, p_u$ of (4) is re-
placed by $f_m^{(n)}(\tilde{R})$ for the acoustic case or by, e.g., $\underline{M}_{-m}^{(n)}(\tilde{R})$
or $\underline{N}_{-m}^{(n)}(\tilde{R})$ of (6') or (6'') for the electromagnetic case.
Since the probe is assumed to directly measure the field
without perturbing it, the probe coefficients (p_u's) are no
longer pertinent.

Equations (7) through (13) and (15) and even the repre-
sentation coefficients are no longer needed (except in an
abstract sense in the following). With the aid of (12) and
a proof analogous to that given by Wigner [p. 115] for finite
groups, it may be shown that

$$\int_R f_m^{(n)}(\tilde{R}) \, g_{m'}^{(n')}(\tilde{R})^* \, \rho(R) \, dR = \delta_{nn'} \, \delta_{mm'} \int_R f_m^{(n)}(\tilde{R}) \, g_m^{(n)}(\tilde{R})^* \, \rho(R) \, dR$$

(12')

is zero unless both n = n' and m = m'; in addition, it is
independent of m, provided that both the f's and g's are
partner functions. In the integration, the variable which is
constant on the scanning surface is fixed.

For the electromagnetic case,

$$\int_R \underline{F}^{smn}(\tilde{R}) \cdot \underline{G}^{s'm'n'}(\tilde{R})^* \, \rho(R) \, dR$$

(12'')

$$= \delta_{nn'} \, \delta_{mm'} \int_R \underline{F}^{smn}(\tilde{R}) \cdot \underline{G}^{s'mn}(\tilde{R})^* \, \rho(R) \, dR,$$

where the $\underline{G}$'s, like the $\underline{F}$'s, may be $\underline{M}$'s or $\underline{N}$'s and in our
applications may differ from the $\underline{F}$'s in normalization or in
the function $\oint$ of the variable held constant during scanning,
say in the type of Hankel function. Again if both the $\underline{F}$'s
and $\underline{G}$'s are partner functions, the integrals are independent
of m.

If a vector field, electric or magnetic, is represented
by $\underline{F}(\tilde{R}) = \sum_{s,m,n} Q^{smn} \, \underline{F}^{s\,mn}(\tilde{R})$, then the application of (12'')
yields

$$\int_R \underline{b}_0^{\prime\prime\prime}(\tilde{R}) \cdot \underline{G}^{s\,\prime mn}(\tilde{R})^* \; \rho(R) \; dR$$

$$\tag{13'}$$

$$= \frac{a_0^{\prime\prime}}{1 - \Gamma^{\prime\prime\prime} \Gamma_L^{\prime\prime\prime}} \sum_s Q^{smn} \int_R \underline{F}^{smn}(\tilde{R}) \cdot \underline{G}^{s\,\prime mn}(\tilde{R})^* \; \rho(R) \; dR$$

which may be used to determine the Q's. The integral on the right hand side $C^{sns\,\prime}$ can commonly be evaluated in closed form (e.g., see section 9). Since the invariant ($\underline{e}_i$) component is zero for the $\underline{M}$'s and has the same symmetry properties as a scalar for the $\underline{N}$'s, (12'), (12"), and (13') apply for the invariant components alone. Further, the transverse components (those orthogonal to $\underline{e}_i$) obey by themselves (12") and (13').

Hence, it is usually convenient to measure two transverse components of $\underline{E}$, two transverse components of $\underline{H}$, or the invariant ($\underline{e}_i$) components of both $\underline{E}$ and $\underline{H}$. The latter gives rise to two independent "scalar" decompositions with complete decoupling. Application of (13') to the transverse components always decouples into sets of no more than two equations in two unknowns. The decoupling is commonly complete, i.e., the factor $\delta_{ss\,\prime}$ occurs on the right hand side of (13'), eliminating the sum. Since $\underline{M}_m^{(n)} \cdot \underline{N}_m^{(n)} = 0$ at every point [Brand, p. 231] if the definitions (6') and (6") are used, decoupling always occurs if the $\underline{M}$'s or $\underline{N}$'s are real [Hamermesh, p. 138 ff]. It also occurs for planar, cylindrical, and spherical scanning [Stratton, p. 395 (17), p. 397 (33) and (34); Stein (6)] (for the cylindrical case with $\underline{e}_i = \underline{e}_z$ if the medium is lossless).

Expressions related to (10) or (11) rather than (12) are also available, but m is then redundant. Equation (12') and its analogs provide innumerable orthogonalities, which are used, e.g., for the computations in Fourier series, Fourier transform, and Hankel transform decompositions.

III. DETAILS OF SPHERICAL SCANNING

6. Basic Equations

We now adapt the general treatment to the spherical case. To the extent feasible, we use the notation of Jensen and our two previous progress reports. However, to include the mismatch correction, receiving as well as transmitting test antennas, non-reciprocal probes, etc., some changes in definitions and notation are made. Because the general treatment of sections 4 and 5 is rather abstract, this discussion of spherical scanning is made rather self-contained, even at the expense of repetition, and of course detailed and specific.

It is assumed that the probe revolves about the test antenna with the z' axis of the (primed) coordinate system $O'r'\theta'\phi'$ fixed in the probe passing through the origin O of the (unprimed) coordinate system $Or\theta\phi$ fixed in the antenna. Neglecting multiple reflections between the probe and antenna, assuming the medium, probe, and antenna are electrically linear, and assuming the medium is homogeneous and isotropic, the complex received amplitude with "probe" t (t = 1,2) is given by

$$W^t(A,\chi_0,\theta_0,\phi_0) = \sum_{\substack{s,m,n \\ \sigma,\mu,\nu}} q^{smn} \underset{\sim}{p}^{\sigma\mu\nu t} \underset{\sim}{g}^{smn}_{\sigma\mu\nu} (A,\chi_0,\theta_0,\phi_0) \quad (14)$$

a special case of (4) (developed in section 4). (One probe with two orientations or two probes are required to determine polarization effects.) To be explicit and in accordance with both the table of section 5.2 and table 1, we express q_M, p_u, and $g_{Mu}(\tilde{R})$ of (4) as q^{smn}, $\underset{\sim}{p}^{\sigma\mu\nu t}$, and $\underset{\sim}{g}^{smn}_{\sigma\mu\nu}(A,\chi_0,\theta_0,\phi_0)$ respectively. For notational simplicity, Jensen's W is redefined as $b_0^{'''}(1-\Gamma^{'''}\Gamma_L^{'''})/a_0^{''}$ where $b_0^{'''}$ is the complex amplitude of the signal delivered to the load of the receiving antenna (probe or test antenna), $a_0^{''}$ is the complex amplitude of the signal fed to the transmitting antenna (test antenna or probe), and $(1-\Gamma^{'''}\Gamma_L^{'''})$ is a mismatch factor, $\Gamma_L^{'''}$ and $\Gamma^{'''}$ being the complex reflection coefficients at the reference plane of the receiving antenna, looking toward the load and antenna respectively with the antenna looking into space. Here ϕ_0, θ_0, and χ_0 are the Eulerian angles which express the orientation of the probe

coordinate system with respect to the antenna coordinate sys-
tem, and A is the distance between the origins of the two
systems. See figure 3. $A = r_0$ is the radius of the scanning
sphere. The q's and p's are the modal coefficients expressing
the patterns of the test antenna and probe respectively, each
in its own coordinate system, whether the transmission be from
the test antenna to the probe or from the probe to the test
antenna. The same modal types, including types of polariza-
tion, are used for the test antenna and probe, such that the
modes are identical for superposed coordinate systems
$(\phi_0 = \theta_0 = \chi_0 = A = r_0 = 0)$. The transmitting pattern T is
used for the transmitting antenna and the receiving pattern
R for the receiving antenna (see (3)). Jensen assumes that
the probe receives and uses its transmitting pattern, not its
receiving pattern, with a reciprocity relation in his g's.
To distinguish, we use p and g rather than p and g, but
otherwise adopt Jensen's notation. Further, modal indices
are used as superscripts and/or subscripts in the manner of
Jensen. The bilinear form of (14) is due to linearity and
the neglect of multiple reflections; the detailed nature of
the g's is due to the symmetry of the spherical modes (see
(16), (15), and Appendix II).

    Of the modal indices, the polarization indices s and σ
each assume the values 1 and 2 for the M and N modes (of
section 5.1) respectively, m and μ express the dependences
of the modes upon the azimuthal angles ϕ and ϕ', and n and ν
(with m and μ) express the dependences upon the polar angles
θ and θ'. As in section 5 and table 1, m and μ indicate rows
and n and ν representations of the (spherical) symmetry
group. For a homogeneous isotropic source-free medium, we
identify the M and N modes of (6') and (6") with TE and TM
modes respectively [Stratton, Chapter VII]. Transverse is
defined relative to spheres centered at the origin of the
given coordinate system, i.e., $\underline{e}_i$ of section 5.1 is $\underline{e}_r$. See
Appendix II for the full description and normalization of
the modes.

    The p's are assumed known from previous measurements of
the probe pattern in its far field (see section 9). The q's
are to be determined from the set of simultaneous equations
(14) and the measured values of W. However, there are two
complex equations for every measurement point, and the g's are
very difficult to compute and seldom zero. For practical data
reduction, the equations must be decoupled and computation of
the g's must be minimized or eliminated.

For a given "probe" t, a given radius A of the scanning (measurement) sphere, and a given frequency, the probe pattern may be transformed once and for all to the origin of the test antenna, namely

$$p^{s\mu nAt} = \sum_{\sigma,\nu} c^{sn}_{\sigma\mu\nu}(A) \; p^{\sigma\mu\nu t}. \tag{15}$$

The c's are simply related to Jensen's C's [pp. 107-112] and this transformation is discussed in detail in Appendix II.

Renormalizing the q's and p's for computational convenience and expressing the angular dependence explicitly, eq. (14) becomes

$$W^{At}(\chi_0,\theta_0,\phi_0) = \sum_{s,m,n} Q^{smn} \sum_{\mu} p^{s\mu nAt} \; e^{im\phi_0} \; d^{(n)}_{m\mu}(\theta_0) \; e^{+i\mu\chi_0}, \tag{16}$$

a special case of (9) which is proved in section 5.2. (Due to the form of (15), we may identify $\bar{\mu}$ with μ. We add the indices A and t to p, P, and W to be explicit.) Equation (16) is a generalization of Jensen's (2.122), (VII.25), renormalized for computational simplicity. That is, the P's and Q's of both (9) and (16) are coefficients of partner functions discussed in section 5.2. The functions may be, e.g., Edmonds spherical harmonics $Y_{mn}(\theta,\phi)$ rather than $P^m_n(\cos\theta) \; e^{im\phi}$ [Edmonds, pp. 53, 54, 59], eliminating Jensen's factor [VII.15] $(-\mu/|\mu|)^\mu \; (-m/|m|)^m \; \{(n+|\mu|)! \; (n-|m|)!/(n-|\mu|)! \; (n+|m|)!\}^{1/2}$ from routine computations. The three angular factors of (16) constitute the representation coefficient $D^{(n)}_{m\mu}(R)$ of (9), here $D^{(n)}_{m\mu}(\phi_0, \theta_0, \chi_0)$ of the spherical point group [section 5; table 1; Edmonds, (4.2.12)]. The d's are truncated Fourier series [Edmonds, (4.5.2)] in θ_0, proportional to associated Legendre functions for $\mu = 0$ or $m = 0$.

Note that we define the Eulerian angles ϕ_0, θ_0, and χ_0 as operations upon the moving probe and its moving coordinate system, leading to (7) which expresses moving (probe) modes in terms of fixed (test antenna) modes. On the contrary, Edmonds [pp. 53-55] and Stein [p. 21] define the Eulerian angles as operating upon a moving coordinate system used to expand a function (mode) fixed in space, giving rise to Edmonds equation (4.1.4) which expands a function fixed in space (test antenna mode) in terms of moving functions (probe modes). Hence, our ϕ_0, θ_0, and χ_0 correspond in this application to

Edmonds $-\chi_0$, $-\theta_0$, and $-\phi_0$ respectively. Although Jensen describes θ_0 and ϕ_0 as position coordinates of the probe [page 36], he nevertheless makes this transcription in his equations (VII.16) and (VII.23). However, in his explicit expression for the F (VII.25), he gives a form inconsistent with his (VII.15) and (VII.16). Moreover, as previously mentioned, he includes a reciprocity relation in his g given in his equations (2.121) and (2.122). Hence our formulas differ from his.

Now

$$\int_0^{2\pi} \int_0^{\pi} \int_0^{2\pi} D_{m\mu}^{(n)}(\phi_0,\theta_0,\chi_0) \; D_{m'\mu'}^{(n')}(\phi_0,\theta_0,\chi_0)^* \left[\frac{\sin\theta_0}{8\pi^2}\right] d\phi_0 d\theta_0 d\chi_0$$

$$= \delta_{nn'} \; \delta_{mm'} \; \delta_{\mu\mu'} / (2n+1) \tag{17}$$

[Edmonds, (4.6.1)], a special case of (12) which is a standard expression. Primes on modal indices are used to indicate another specific value, not a coordinate system or antenna. Hence, multiplication of (16) by $D_{m'\mu'}^{(n')}(\phi_0, \theta_0, \chi_0)^* (\sin\theta_0)/8\pi^2$ and integration reduces (16) to

$$\frac{1}{8\pi^2} \int_0^{2\pi} \int_0^{\pi} \int_0^{2\pi} W^{At}(\phi_0,\theta_0,\chi_0) \; D_{m'\mu'}^{(n')}(\phi_0,\theta_0,\chi_0)^* \sin\theta_0 \; d\phi_0 d\theta_0 d\chi_0$$

$$= (Q^{1m'n'}P^{1\mu'n'At} + Q^{2m'n'}P^{2\mu'n'At})/(2n+1) \tag{18}$$

a special case of (13). Thus, the simultaneous equations (16) have been reduced to sets of two equations (for two "probes") in two unknowns (Q's).

7.   Probe Design

Since the integrations over ϕ_0 and χ_0 are essentially finite Fourier series decompositions due to the exponentials of D (see table 1 and (16)), the totality of the integrations over ϕ_0 and χ_0 (for all m' and μ') are easily carried out without approximation (except for possible aliasing) as a single two dimensional Fast Fourier "Transform." However, by proper probe design, it is possible to eliminate measurements (and computation) as a function of χ_0, reduce the number of P's necessary to express the probe pattern, and reduce the required number of D's to those for one or two μ

28

values. Moreover, as will be shown, it is unnecessary to compute the D's or to carry out ordinary numerical integration over ϕ_0, θ_0, or χ_0.

Specifically, if the probe is circularly (azimuthally) symmetric in the material sense and its leads (e.g., waveguide) propagate only a single mode, the μ value is determined, eliminating measurements and integration as a function of χ_0. The probe may have arbitrary variation of its cross section with length (e.g., arbitrary flare), leading to an arbitrary dependence of the probe pattern upon its polar angle θ'.

For the TE_{01} mode of circular guide (t = 1) and the TEM mode of coaxial guide (t = 2), $\mu = 0$. The first probe responds only to spherical TE modes ($\sigma = 1$) and the second to only spherical TM modes ($\sigma = 2$), regardless of fringing as may be seen in figure 4. Qualitatively they respond to the radial components of $\underline{H}$ and $\underline{E}$ respectively. Although such probes are quite impractical in the far field, they may be quite practical for the very near field, as James and Longdon's measurements of the radial electric field show. Since $c_{\sigma\mu\nu}^{sn}(A)$ of (15) for $\mu = 0$ is zero if $s \neq \sigma$ (see Appendix II), we may set $s = \sigma = t$ and this procedure results in complete separation of the unknowns (Q's). (Modes other than the TE_{01} mode in circular guide may be suppressed with vanes, a TE_{01} guide 1 km long being under construction in Japan.)

For an arbitrary distance from the test antenna, the lowest mode of circular guide (the TE_{11} mode) may be used or alternatively a thin dipole short compared to a half a wavelength. For such probes, $\mu = \pm 1$. They measure essentially the transverse electric field and respond to both TM and TE spherical modes.

The pattern of each aforementioned probe has precisely the same azimuthal (ϕ') dependence as that of an ideal dipole, while the commonly used rectangular guide probes must have high order multipole constituents just to meet the cross-sectional boundary conditions. Hence, small probes of the aforementioned types would be expected to provide quite good approximations to ideal dipoles. The case of no probe correction is discussed in section 9.

8. Computation of the Test Antenna Pattern Coefficients (Q's)

For the probe correction case with a probe used to measure the transverse electric field, the data are desired in the "circular" polarization representation ($e^{+i\mu\chi_0}$, $\mu = \pm 1$),

29

rather than the "linear" representation ($\cos \mu\chi_0$, $\sin |\mu| \chi_0$), as may be seen from (16). However, since probes designed to receive a single "circular" polarization tend to be quite frequency dependent, a probe designed to receive "linear" polarization is used. For a circular waveguide probe, a circular to rectangular waveguide transition may be used and/or a vane used in the circular guide to fix the polarization. In any event, the circular guide should be long enough and of such a diameter as to propagate only the TE_{11} mode. Then from eq. (16), the complex received signal corresponding to $\mu = \pm 1$ is given by

$$W(\mu = \pm 1) = \frac{1}{2}[W(\chi_0 = 0) \pm iW(\chi_0 = \pi/2)], \qquad (19)$$

where χ_0 is the Eulerian angle describing the rotation of the probe about its own axis. Thus, a FFT with respect to ϕ_0, coupled with eq. (19) for transverse component probes, reduces (16) to sets of equations of the form

$$W^{m\mu At}(\theta_0) = \sum_{s,n} Q^{smn} P^{s\mu nAt} d_{m\mu}^{(n)}(\theta_0)$$

$$= \sum_{s=1}^{2} \lfloor d_{m\mu}^{(n)}(\theta_0) \rfloor \; \{Q_n^{sm} P_n^{s\mu At}\}, \qquad (20)$$

where m and μ are known, t is needed only for the $\mu = 0$ case, and $n \geq |m|, |\mu|$. We use matrix notation to relate the analysis more closely to the required computer programming. Broken brackets are used to indicate a row matrix and curly brackets to indicate a column matrix. In the following, indices which indicate rows and columns are lowered to the subscript position; where this is impractical, the index is encircled.

Separation according to the n value is conceptually based upon the orthogonality of the d's, namely

$$\int_0^\pi d_{m\mu}^{(n)}(\theta_0) \; d_{m\mu}^{(n')}(\theta_0) \sin\theta_0 \; d\theta_0 = \delta_{nn'}/(n+\tfrac{1}{2}), \qquad (21)$$

a special case of (17) utilizing the definition of the D's in (16). The integration is one dimensional since separation according to m and μ has already been achieved. Hence, pre-multiplying both sides of (20) by the column matrix $\{d_{m\mu}^{(n)}(\theta_0) \sin\theta_0\}$ and integrating, one obtains

30

$$\int_0^\pi \{d_{m\mu}^{(n')}(\theta_0)\ \sin\theta_0\}\ W^{m\mu At}(\theta_0)\ d\theta_0$$

$$= \sum_{s=1}^{2} \int_0^\pi \{d_{m\mu}^{(n')}(\theta_0)\ \sin\theta_0\}\ \lfloor d_{m\mu}^{(n)}(\theta_0)\rfloor\ \{Q_n^{sm}\ P_n^{s\mu At}\}\ d\theta_0$$

$$= \sum_{s=1}^{2} \{Q_n^{sm}\ P_n^{s\mu At}/(n+\tfrac{1}{2})\}\delta_{nn'}, \tag{22}$$

since the integration over the θ_0 matrices yields a diagonal matrix with diagonal elements $1/(n+\tfrac{1}{2})$. Thus, the simultaneous equations represented by (16) have been split into sets of two equations in two complex "scalar" unknowns Q^{1mn} and Q^{2mn}. For the transverse probes, there are two equations for $\mu = +1$ and -1, while for the radial $\mu = 0$ probes, two physical probes are used, $t = s$, and the decoupling of the equations is complete.

However, we wish to avoid the computation of the d's and the numerical integration implied by the left hand side of (22). To evaluate the left hand side of (22), we express both $W^{m\mu At}(\theta_0)$ and the elements of $\{d_{m\mu}^{(n)}(\theta_0)\ \sin\theta_0\}$ as Fourier series. Since $W^{m\mu At}(\theta_0)$, like the $d_{m\mu}^{(n)}(\theta_0)$'s, is even or odd in θ_0 as $m-\mu$ is even or odd (see Appendix I), the values for negative θ_0 may be filled in and an ordinary FFT carried out. Since the values for negative θ_0 are introduced only during the computation for a given m and μ, they add little to the computer storage problem. Thus, FFT's are carried out over ϕ_0 for each non-negative θ_0 value followed by FFT's over θ_0 for each m value, rather than a two-dimensional FFT; however, the number of multiplications is identical. This yields $W^{m''m\mu At}$, where

$$W^{m\mu At}(\theta_0) = \lfloor e^{im''\theta_0}\rfloor\ \{W_{m''}^{m\mu At}\}. \tag{23}$$

Since $d_{m\mu}^{(n)}(\theta_0)$ is given by a sine or cosine Fourier series of order n with real constant coefficients (see Appendix I), $\{d_{m\mu}^{(n)}(\theta_0)\ \sin\theta_0\}$ is given by the product $[f_{nm'}^{m\mu}]$

$\{e^{im'\theta}0\}$ where m' runs from -n-1 to +n+1. The indices m and μ on the first matrix merely indicate which rectangular matrix is involved. Thus, the left side of eq. (22) becomes

$$\int_0^\pi [f_{nm'}^{m\mu}] \ \{e^{im'\theta}0\} \ \lfloor e^{im'\theta}0 \rfloor \ \{W_{m''}^{m\mu At}\} \ d\theta_0$$

(24)

$$= [f_{nm'}^{m\mu}] \ [\Pi_{m'm''}] \ \{W_{m''}^{m\mu At}\},$$

where the elements of Π are equal to π for m'+m" = 0, equal to 2i/(m'+m") for m'+m" odd, and equal to zero if m'+m" is even but not zero. Thus, (22) becomes

$$\{W_n^{m\mu At}\} = [F_{nm''}^{m\mu}] \ \{W_{m''}^{m\mu At}\}$$

(25)

$$= \sum_{s=1}^{2} \ \{Q_n^{sm} \ P_n^{s\mu At}/(n+\tfrac{1}{2})\}$$

(26)

where $[F_{nm''}^{m\mu}] = [f_{nm'}^{m\mu}][\Pi_{m'm''}]$. Both the [f]'s and [F]'s are constant matrices with all the elements either pure real or pure imaginary. Computation of [f] is described in Appendix I.

The forward "multiplying matrix" $[F_{nm''}^{m\mu}]$ is computed for each value of μ (zero or +1 and -1) and each value of m, the number of m values being no greater than the number of ϕ_0 values used on a latitude. As previously noted, the matrices are independent of the frequency, the test antenna, the choice of measurement points, the detailed nature of the probe(s) t, and the radius r_0 = A of the scanning sphere, although the μ value(s) depend upon the probe type(s) and the appropriate number of m values depends upon the fine structure of the antenna pattern. Hence the [F]'s need to be computed only once.

Actually, the computation implied by (24) may be con-siderably simplified by symmetry analysis analogous to that which justifies writing

$$\int_{x=-a}^{a} \int_{y=-b}^{b} f(x,y) \ e(x) \ o(y) \ dx \ dy$$

$$= 4 \int_{x=0}^{a} \int_{y=0}^{b} f_{eo}(x,y) \ e(x) \ o(y) \ dx \ dy,$$

where $e(x)$ is an even function, $o(y)$ is an odd function, and $f_{eo}(x,y)$ is that part of $f(x,y)$ which is even with respect to x and odd with respect to y [Hamermesh (3-184), table 4-11, C_{2v}]. This shows that the cross-diagonal ($m'+m'' = 0$) terms of Π do not contribute and that the matrix elements for negative m' or m'' are unneeded. Thus, the f's for negative m' need not be computed or used, the W's for negative m'' are not used, and Π is replaced by a quadrant submatrix of the appropriate constituent of Π (eo or oe).

The previously described computations thus yield two equations ($\mu = +1, -1$) in two unknowns (Q's). The equations are easily solved for the Q's, assuming the P's (discussed in Appendix II) are known. (For the $\mu = 0$ probes, the separation occurs with the probe, namely $t = s$.)

9. Data Processing Without Probe Pattern Correction;

Determination of Probe Pattern

As mentioned in section 5.5, the data reduction is markedly simplified if a probe pattern correction is not required. In particular, the translational transformation (15) is eliminated. In this approximation, two of the spherical ($\underline{e}_r$, $\underline{e}_\theta$, $\underline{e}_\phi$) components of the field are measured directly.

In a flow-chart sense, the data processing is much the same as for the case with probe correction. Equation (16) for the measured field is replaced by the vector equation

$$\underline{W}^A(\theta,\phi) = \sum_{s,m,n} Q^{smn} \underline{F}^{smnA}(\theta,\phi) \tag{16'}$$

where the $\underline{F}$'s are defined in section 5.1 and we no longer need to distinguish between θ and θ_0 or between ϕ and ϕ_0. The decomposition equation (18) is replaced by

$$\int_{\theta=0}^{\pi} \int_{\phi=0}^{2\pi} \underline{W}^A(\theta,\phi) \cdot \underline{G}^{smn}(\theta,\phi)^* \sin\theta \, d\theta d\phi \tag{18'}$$

$$= Q^{smn} \int_{\theta=0}^{\pi} \int_{\phi=0}^{2\pi} \underline{F}^{smn}(\theta,\phi) \cdot \underline{G}^{smn}(\theta,\phi)^* \sin\theta \, d\theta d\phi,$$

a special case of (13') of section 5.5. (Primed equation numbers are used to display correspondences.) The integration over χ_0 implied by (13') merely introduces the (cancelled) factor 2π since the integrands are independent of this variable,

$\underline{b}_0'''$ and $\underline{W}^A$ just being representations of the actual complex vector field of the test antenna. (Although discussion is sometimes in terms of a transmitting test antenna for convenience, this section, like the rest of this report, applies equally well to a receiving test antenna.) Further, an analog of the μ decomposition (19) is unneeded; the indices μ and t no longer occur. As mentioned in section 5.5, the $\underline{M}$ and N functions are orthogonal for the spherical case [Stein (6)], so that the decoupling is complete.

So that the right hand side will be independent of m, we base the G's upon partner functions rather than $P_n^m(\cos\theta)e^{im\phi}$ (see sections 5.2 and 6). For brevity, we confine our further discussion to the more complicated but important case of transverse component measurement. Since (18') is a special case of (13') which holds for the transverse components alone (as discussed in section 5.5), we choose $\underline{G}$'s without $\underline{e}_r$ components and suppress such components in both $\underline{W}^A$ and $\underline{F}^{smnA}$ of (16') and (18') and in the remainder of this section. We define $\underline{G}^{1mn}(\theta,\phi) = (-1)^m e^{im\phi}(A^{mn}\underline{e}_\theta - B^{mn}\underline{e}_\phi)$ and $\underline{G}^{2mn}(\theta,\phi) = (-1)^m e^{im\phi}(B^{mn}\underline{e}_\theta + A^{mn}\underline{e}_\phi)$ where $A^{mn} = im\,d_{m0}^{(n)}(\theta)/\sin\theta$ and $B^{mn} = d(d_{m0}^{(n)}(\theta))/d\theta$. Thus, we make use of the d's required for data processing with probe correction rather than introducing additional functions such as Edmond's spherical harmonics (Y's) [Edmonds, (4.1.25)].

For the $e^{im\phi}$ dependence which we use, the Fourier series decomposition with respect to ϕ is easily carried out (for each non-negative θ) by means of an FFT, reducing (16') to sets of vector equations of the form

$$\underline{W}^{mA}(\theta) = \sum_s \lfloor \underline{F}_n^{smA}(\theta) \rfloor \{Q_n^{sm}\}, \tag{20'}$$

where m is known, $n \geq |m|$, and $\underline{F}^{smnA}(\theta)$ is the coefficient of $e^{im\phi}$ in the Fourier series expansion of $\underline{F}^{smnA}(\theta,\phi)$. Premultiplying both sides of (20') by the column matrix $\{G_n^{s'm}(\theta)^*\sin\theta\}$, we obtain

$$\int_0^\pi \{\underline{G}_n^{s'm}(\theta)^* \sin\theta\}\cdot\underline{W}^{mA}(\theta)\,d\theta$$

$$= \sum_s \int_0^\pi \{\underline{G}_n^{s'm}(\theta)^* \sin\theta\}\cdot\lfloor\underline{F}_n^{smA}(\theta)\rfloor\{Q_n^{sm}\}\,d\theta \tag{22'}$$

$$= \{C_n^{sA}Q_n^{sm}\}\,\delta_{ss'}\delta_{nn'}$$

34

where $\underline{G}^{smn}(\theta)$ is the coefficient of $e^{im\phi}$ in the Fourier series expansion of $\underline{G}^{smn}(\theta,\phi)$ and $C^{snA} = \int_0^{2\pi} \underline{F}^{smnA}(\theta) \cdot \underline{G}^{smn}(\theta)^* \sin\theta\, d\theta$, the integral being independent of m, zero for $s \neq s'$ or $n \neq n'$ [section 5.5], and available in closed form [Stratton, p. 417 (20)]. Thus, complete decoupling has been achieved.

To avoid both the evaluation of the $\underline{G}$'s as functions of θ and ordinary numerical integration, we proceed as with (22), i.e., we express the left hand side of (22') in terms of Fourier series. The A's and B's are odd functions of θ for even m and even functions of θ for odd m (see Appendix I). Moreover, both the A's and B's are given by Fourier series of order n (see Appendix I and Stratton p. 401 (12), noting that $A = 0$ if $m = 0$). Thus, we may write $\{A_n^m(\theta)\} = [a_{nm'}^m]\{e^{im'\theta}\}$, $\{B_n^m(\theta)\} = [b_{nm'}^m]\{e^{im'\theta}\}$, and $\{\underline{G}_n^{sm}(\theta)^* \sin\theta\} \equiv [g_{nm'}^{sm}]\{e^{im'\theta}\}$, where for each s and m, the elements of the $\underline{G}$'s and g's are two-vectors and m' of the last equation runs from $-n-1$ to $n+1$. The a's, b's, and g's may be evaluated like the f's described in Appendix I. Further, a development analogous to that in section 8 leads to

$$\{W_n^{smA}\} = [\underline{G}_{nm''}^{sm}] \cdot \{\underline{W}_{m''}^{mA}\} \qquad (25')$$

$$= \{Q_n^{sm} C_n^{sA}\}, \qquad (26')$$

where $[\underline{G}_{nm''}^{sm}] = [g_{nm'}^{sm}][\Pi_{m'm''}]$. Note that the elements of both the left hand side of (25') and the right hand side of (26') are "scalars" (matrices with a single row and column) and that the decoupling is complete, not merely into sets of two equations in two unknowns (Q's). As in computing $\{W_{m''}^{m\mu At}\}$ from $W^{m\mu At}(\theta_0)$ in section 8, so in computing $\{\underline{W}_{m''}^{mA}\}$ from $\underline{W}^{mA}(\theta)$, the values of $W^{mA}(\theta)$ for negative θ are filled in according to whether m is even or odd.

The preceding treatment is convenient for determining the probe pattern coefficients (p's). The probe is scanned on a spherical surface in its far field with a standard probe of known polarization, preferably linear. Hence, for a normal type standard probe, only its on-axis properties are required and it may be considered to be an ideal electric dipole ($\sigma = 2$, $\mu = \pm 1$, $\nu = 1$) since it essentially measures the field of the probe at a point on the measurement sphere. If absolute values and the ultimate in accuracy are required,

35

the properties of the standard probe may be determined by
the three antenna method [Newell, Baird, and Wacker]. If
only relative values are needed and the standard probe may
be assumed to have a known linear polarization, no measure-
ments of the standard probe or of the load mismatch factor
are required. Since the measurement probe always faces the
test antenna, information concerning its pattern is required
only for the facing hemisphere ($\pi \geq \theta' \geq \pi/2$). Further, for
large separations between the probe and test antenna, the
pattern well off axis (θ' near $\pi/2$) is relatively unimportant.

10. Statistical Considerations

If the number of Q's is equal to twice the number of
measurement points, the data will usually be fitted exactly,
including random experimental error. However, it is desirable
to discriminate against random error as one does in drawing a
rather smooth curve through 1000 data values, say by using a
polynomial of moderate degree rather than degree 999. One
may similarly discriminate here by using a smaller number of
Q's, say by leaving out those corresponding to the higher n's
and m's, these corresponding to a rapid angular variation
which is not realistic outside the reactive zone of the an-
tenna. This may be done arbitrarily, or the Fisher-Snedecor
F test of statistical significance [Bennett and Franklin,
pp. 108-110, 192 ff.] may be used, as in the NBS extrapolation
method. Even better, one may plot weighted squares of the
magnitudes of the Q's as functions of n and m, omitting those
down in the noise. The latter methods provide statistical
justification for the choice of individual Q's, throwing out
those Q's for which the square of its magnitude is below a
simple criterion. Our formulation has the advantage that it
gives least square values of the Q's, regardless of the set
of Q's chosen--least square in the sense that the sum of the
squares of the magnitudes of complex deviations of the fitted
from the experimental near-field data, weighted with the fac-
tor $\sin \theta_0$, is minimized. Jensen's original procedure requires
as many Q's as measurements and does not give least squares
values. (For the probe correction and no probe correction
cases, the aforementioned weighted squares are
$|Q^{smn} P^{s\mu nAt}/\sqrt{N_n}|^2$ and $|Q^{smn} \sqrt{C^{snA} g^{snA*}}|^2$ respectively, where
$g^{snA} \equiv F^{smnA}/G^{smn}$. These squares are appropriate due to the
properties of orthonormal functions [Riesz and Sz.-Nagy, p. 66],
$\sqrt{N_n} D_{m\mu}^{(n)}$ and $F^{smnA}/\sqrt{C^{snA} g^{snA*}}$ being orthonormal in the sense
of the scalar product of a Hilbert space [Riesz and Sz.-Nagy,
p. 198]. (See (12), (17), and (12"), noting that the integral
on the right hand side of (12") is zero for the spherical case

unless s = s'. For simplicity, it may be convenient to sum
over μ and/or s and then test for the joint significance of
combinations of functions.

11. Computation of the Far Field

For an electrically large antenna, there are many sig-
nificant Q's and the pattern values are usually required for
many directions; hence, an efficient procedure for the compu-
tation of the far field is needed. In particular, we wish to
avoid ordinary evaluation of the many F^{smn}'s as functions of
θ and ϕ. Again we use a matrix multiplication and a two-
dimensional FFT. In (20'), we expand $\underline{W}^{mA}(\theta)$ as $\left\lceil e^{im''\theta} \right\rfloor \{\underline{W}^{mA}_{m''}\}$
as in (23) and in addition expand $\underline{F}^{smA}_n(\theta)$ as $\left\lceil e^{im''\theta} \right\rfloor [\underline{F}^{smA}_{m''n}]$,
showing that

$$\{\underline{W}^{mA}_{m''}\} = \sum_{S} [\underline{F}^{smA}_{m''n}] \{Q^{sm}_n\}. \tag{27'}$$

That is, (27') is the two dimensional Fourier "transform" of
the field. For the far field, we use the asymptotic expansion
for the Hankel functions and divide out the factor $e^{\pm ikr}/kr$
from both sides of (27'). Thus, we find that the "far field"
is the two dimensional inverse FFT of

$$\{\underline{w}^{m}_{m''}\} = \sum_{S} [\underline{B}^{sm}_{m''n}] \{Q^{sm}_n\}, \tag{28'}$$

where the backward multiplying matrix $[\underline{B}^{sm}_{m''n}]$ is defined as
$[\underline{F}^{smA}_{m''n}]$ $kr/e^{\pm ikr}$ where A = r is large. $\underline{B}$ is computed by tech-
niques analogous to those of Appendix I. In fact, except for
the difference in normalization of the $\underline{F}$'s and $\underline{G}$'s -- roughly
the $e^{\pm ikr}/kr$ factor for large r, $[\underline{F}^{smA}_{m''n}]$ is the complex trans-
pose of $[\underline{g}^{sm}_{nm''}]$, which is the matrix corresponding to $[\mathcal{g}]$ of
Appendix I, i.e., the matrix obtained in calculating $[g^{sm}_{nm''}]$,
just before modification to include the sin θ factor. The
elements of the first two matrices of (27') and of (28') are
complex two-vectors.

If a probe correction is used to obtain the Q's and com-
puter storage is a problem, an alternative but parallel com-
putation may be used to avoid introducing the $\underline{B}$'s. $W^{m\mu At}$ and
$\left\lceil d^{(n)}_{m\mu}(\theta_0) \right\rfloor$ of (20) are expanded as $\left\lceil e^{im''\theta_0} \right\rfloor \{W^{m\mu A\bar{t}}_{m''}\}$ and

$\left[e^{im''\theta}\mathbf{0}\right]$ $[D^{m\mu}_{m''n}]$ respectively. Since ideal dipoles give a field component at a point, we use transverse ideal dipoles as hypothetical probes in the far field computations, indicating this with an overline. Making the preceding substitutions in (20) yields

$$\{\overline{W}^{m\mu A}_{m''}\} = \sum_{s} [D^{m\mu}_{m''n}] \{Q^{sm}_{n} \overline{P}^{s\mu A}_{n}\}. \qquad (27)$$

Dividing through by $e^{\pm ikr}/kr$, one obtains

$$\{\overline{w}^{m\mu}_{m''}\} = \sum_{s} [D^{m\mu}_{m''n}] \{Q^{sm}_{n} \overline{P}^{s\mu}_{n}\} \qquad (28)$$

with obvious definitions. The p's are not to be confused with those of (4) or (14) for actual probes. The p's of (28) may be computed with expressions for the c's of (15) given in Appendix II. (As mentioned in section 9, for transverse ideal electric dipole, $\sigma = 2$, $\mu = \pm 1$, and $\nu = 1$.) The D's are Hermitian conjugates (complex transposes) of the $[\delta^{m\mu}_{nm'}]$ of Appendix I; thus the δ's may be fed into the computer and used for the computation of both the Q's and the far field. The FFT of (28) yields the far field in the circular polarization representation; to obtain the far field in the θ, ϕ representation, the inverse of (19) may be applied to the left hand side of (28) prior to performing the FFT.

By a simple artifice, the far field may be readily computed for arbitrarily fine spacing in θ and ϕ (submultiples of 2π). One chooses the number of θ values (θ spacing) and the number of ϕ values (ϕ spacing) desired. Since the FFT and its inverse require as many input as output values, zeros are added if necessary to the $w^{mm''}$'s of (28') for missing higher values of $|m|$ and $|m''|$. The inverse FFT then yields least squares values of the far field corresponding to the retained (say statistically significant) Q's. The proposed computations yield the phases and amplitudes of the $\underline{e}_{\phi}$ and $\underline{e}_{\theta}$ components; if the polarization is desired in another representation, it is easily calculated on a modern computer with no loss in accuracy (see section 12). Note that no matrix inversion is required even to obtain the auxiliary matrices $[F^{m\mu}_{nm''}]$, $[\underline{G}^{sm}_{nm''}]$, $[\underline{B}^{sm}_{m''n}]$, and $[D^{m\mu}_{m''n}]$.

12. Experimental Details and Options; Probe Rotation and Polarization Measurements

The preceding analysis assumes that the probe moves about a fixed antenna. Further, for both the probe correction and no probe correction cases, no rotation of the probe about its own axis is assumed, i.e., χ_0 is assumed to be fixed at either 0 or $\pi/2$. For $\phi_0 = \theta_0 = \chi_0 = 0$, x', y', and z' of the probe coordinate system Ox'y'z' have the same directions as x, y, and z respectively of the test antenna coordinate system Oxyz. If χ_0 is held fixed at $\chi_0 = 0$ and ϕ_0 and θ_0 varied, the x', y', and z' directions become the θ, ϕ, and r directions respectively of the test antenna coordinate system. Thus, an ideal dipole originally in the x' direction will measure the θ component for $\chi_0 = 0$ and the ϕ component for $\chi_0 = +\pi/2$.

We wish to relax both the fixed antenna and fixed χ_0 conditions. The probe transport (revolution) system may be eliminated if the antenna is mounted on a conventional antenna rotator (model mount, azimuth over elevation, or elevation over azimuth). Alternatively, the probe transport may be reduced to motion on a semicircle if the antenna is rotated azimuthally. Since the measurements are required for a constant radius, the axes of rotation must intersect as in the model mount or in the WPAFB TAPA scanning system. In the latter system, the antenna rotates about a vertical axis and the probe revolves on a gantry arm with a horizontal axis.

A model mount, like a TAPA-type scanner, has a number of advantages for "spherical" scanning. First, the antenna may be scanned over almost 4π steradians. Further, the scanning center may be chosen close to the "phase center," possibly minimizing the required number of basis functions and so minimizing the required number of measurement points. For a directional antenna, the type of mechanical scanning can reduce the required amount of absorbing material. Thus, a planar wall or ceiling of absorber may be sufficient for a fixed antenna with a movable probe or even for a TAPA system. Since the antenna axis is kept horizontal in the model mount, a cylindrical absorbing wall (say a hemicylinder) may be sufficient for it. However, the wall should extend far enough above and below the antenna so that wide-angle radiation does not pass out the top or bottom and then be reflected back to the probe. Of course, the closer the absorber, the less is required. Further discussion is confined to the model mount and TAPA type scanner, to which the preceding analysis is easily applied if the probe is not rotated about its own axis.

For the model mount and the TAPA scanning system, both mounting and expression of the far field power pattern are convenient if the figure axis of the antenna is taken as the z axis (horizontal axis in the case of the model mount). Further, the polarization is conveniently expressed in these coordinates for a circularly polarized antenna. Moreover, if the test antenna has a good approximation to ϕ or θ, polarization, it may be possible to measure the principal polarization with a linearly polarized probe and neglect the cross polarization. Furthermore, for these types of nominal polarization, high relative accuracy in the cross polarization is possible because it is measured directly, not as the difference of two large numbers.

However, for an antenna with linear polarization (normal to the x or y axis) expression of the polarization in terms of θ and ϕ components is inconvenient, and measurement of a small cross polarization tends to be inaccurate for fixed χ_0. Hence, we generalize the previous treatment to permit rotation of the probe about its own axis, still avoiding measurement and data processing as functions of three Eulerian angles. In (16) we take $\chi_0 = \alpha \, \phi_0 + \beta$ where α is an integer (say 0 or ± 1) and β is 0 or $\pi/2$. Thus, the angular part of (16) becomes $e^{i \, (m+\alpha\mu)\phi_0} \, d_{m\mu}^{(n)}(\theta_0) \, e^{+i\mu\beta}$. Hence, the μ separation (for fixed ϕ_0) may be carried out as before, replacing χ_0 in (19) by β. Since the received signal depends upon ϕ_0 as if m were replaced by $m+\alpha\mu$, the FFT with respect to ϕ_0 is carried out as before, but correction for the shift in the m value needs to be carried out prior to extending the data to negative θ_0 and taking the FFT with respect to this variable. Hence, rotation of the probe about its axis may be used to increase the accuracy of the cross polarization measurements without significantly increasing or changing the computations.

Regardless of probe rotation and therefore regardless of the polarization representation used in the actual measurements, the computations are carried out in the ϕ, θ representation. However, this causes no degradation in the accuracy of the far field, due to the number of significant figures carried in a modern computer. That is, even if $W(\beta = \pi/2)$ is so small that the difference between $W(\mu = 1)$ and $W(\mu = -1)$ is less than their individual uncertainties, the full accuracy in both $W(\beta = 0)$ and $W(\beta = \pi/2)$ is carried implicitly. Thus, it is quite unnecessary to replace [F] of (25) and [G] of (25') by matrices corresponding to cos and sin χ_0 rather than $e^{\pm i\chi_0}$, although this would be possible.

13. Relation to Planar Measurements and Data Processing

Since the required measurements for both the spherical and planar scanning procedures are phase and amplitude outputs of each of two "probes" t on an array equally spaced in the two position coordinates, the instrumentation (apart from antenna rotation and/or probe positioning) and initial parts of the computer programming are almost identical. For example, the same system may be used for measurement triggering, phase and amplitude measurement, analog-to-digital conversion, sample and hold, tape formatting, computer input, calibration corrections, and drift corrections (renormalization using tie scans). Further, the Fast Fourier Transform processing is much the same.

The latter requires that the measurements be equally spaced in the two coordinates. However, unlike the planar case, the spacing cannot be arbitrary. In both the spherical and circular cylindrical cases, the spacings of the angular variables must be integral submultiples of 2π. Nevertheless, for directions of negligible radiation, the W's may be arbitrarily set equal to zero without measurement.

A tentative flow chart for the spherical case with probe correction is given in figure 6.
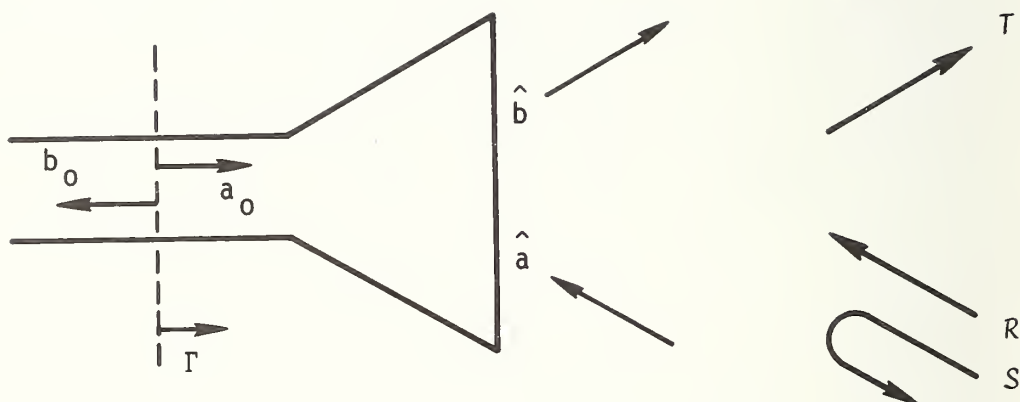
Figure 1. Complex wave amplitudes and scattering matrix
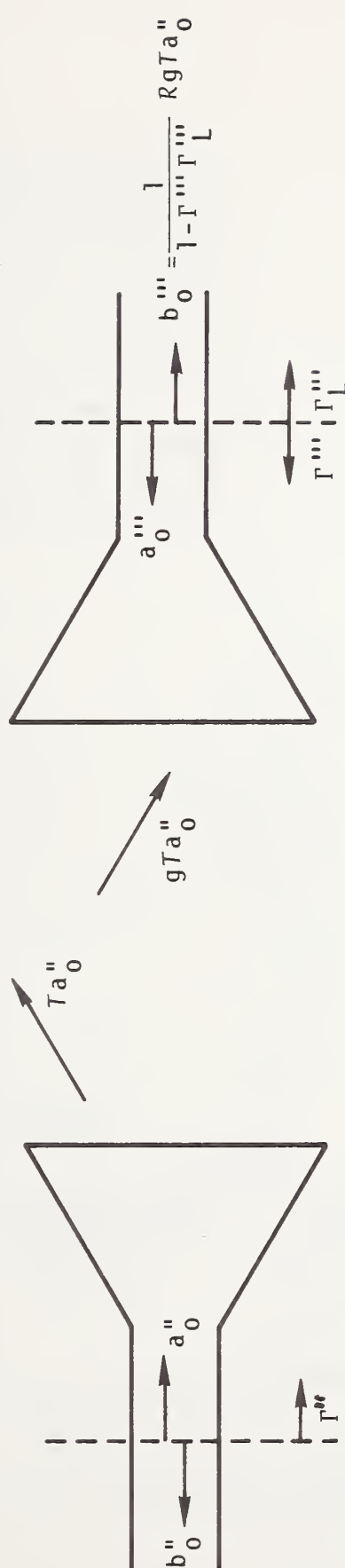elements of an antenna.

Figure 2. An antenna pair showing complex wave amplitudes and scattering matrix elements. The amplitude b_0''' delivered to the load of the receiving antenna is expressed schematically in terms of the amplitude a_0'' fed to the transmitting antenna, its transmitting pattern, the coordinate transformation g, the receiving pattern of the receiving antenna, and the mismatch factor complex $1/(1-\Gamma'''\Gamma'''_L)$.

Figure 3. Eulerian angles of the probe relative to the test antenna. In order, the rotations are ϕ_0 about z to yield $0x_1y_1z_1$, θ_0 about y_1 to yield $0x_2y_2z_2$, and χ_0 about z_2 to yield $0x'y'z_2$; translation by A along z_2 yields z'. Note that the probe faces the negative z', z_2 direction while the test antenna faces a positive direction, say that of $z = z_1$.

$$00' = z_2 - z' = A$$

44
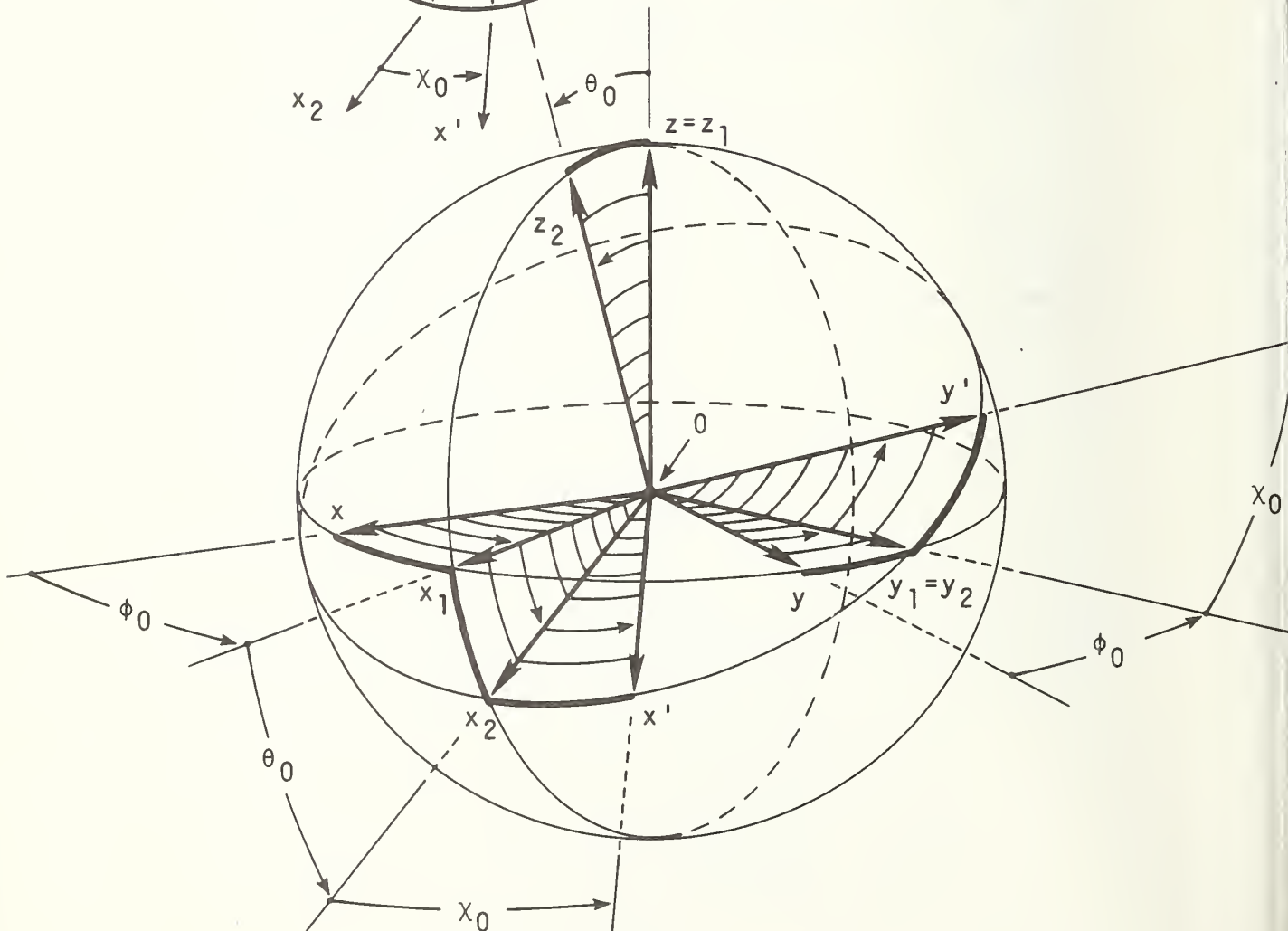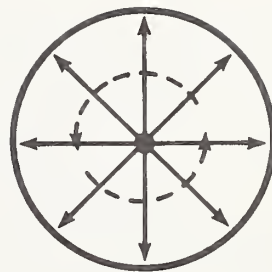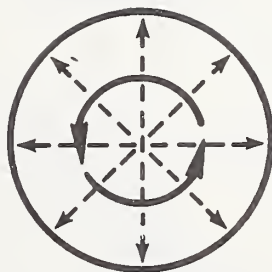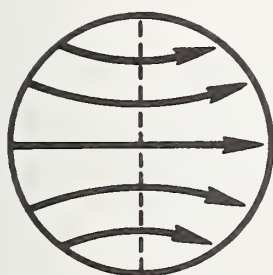
	Waveguide mode		
Waveguide mode	TE_{11}	TE_{01}	TEM
Spherical modes	TE,TM	TE	TM
σ	1,2	1	2
μ	-1,+1	0	0
Component measured (Qualitative)	E_t	H_r	E_r

Figure 4. Probe type and modes. An ideal electric dipole has a TM spherical mode ($\sigma = 2$) and measures E_t; a linear ideal electric dipole has a linear combination of $\mu = -1$ and $\mu = +1$ modes.
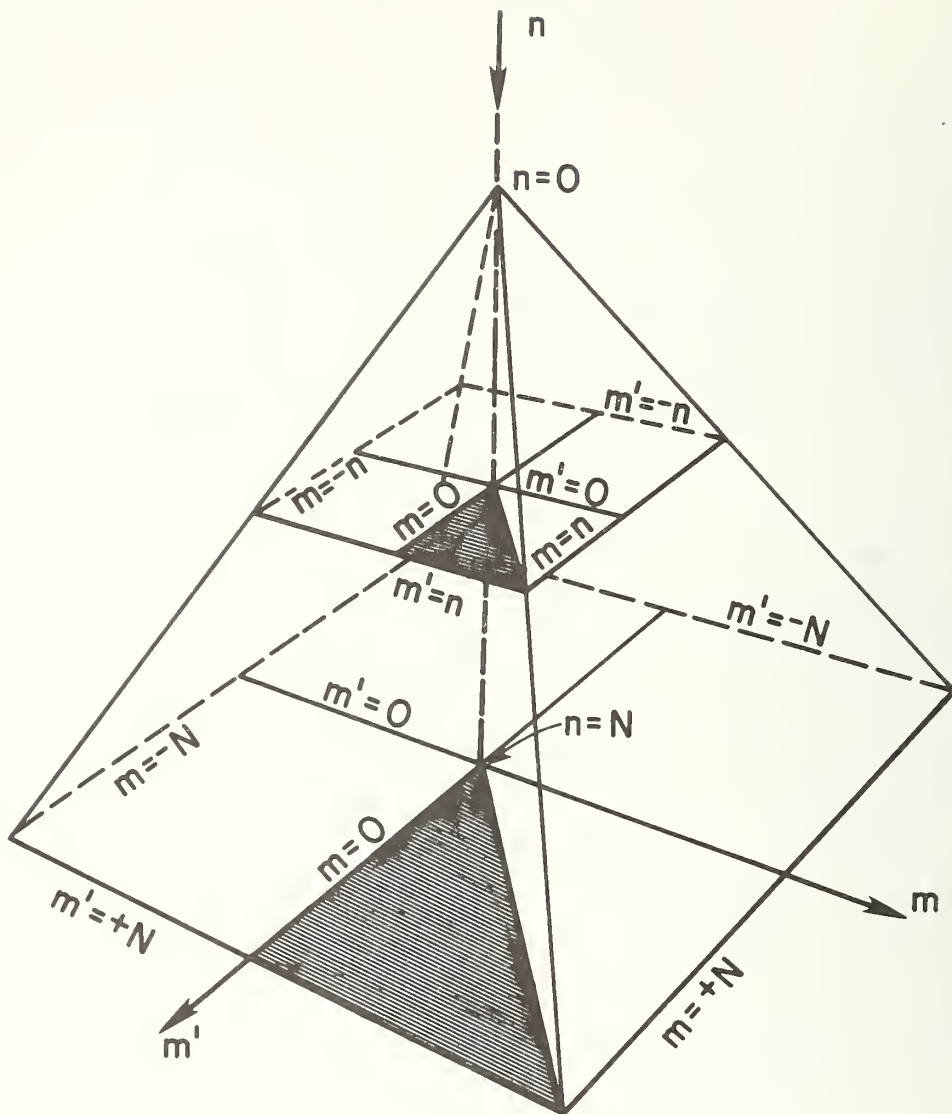
45

Figure 5. Array of $\Delta_{m'm}^{(n)}$'s required for the computation of the multiplying matrix $[F_{nm''}^{m\mu}]$. All the values for a given horizontal plane (n value) may be obtained by simple symmetry relations from those in the shaded octant.

46

Spherical Scanner Data Processing Flowchart
Probe Correction Case

Fig. 6 Flow
for t

NOTES:

1. THE NOTATION OF THE TEXT (AS DESCRIBED IN SECTION 8) IS UTILIZED FOR DESIGNATING MATRIX AND SCALAR QUANTITIES. (E.G.; SUPERSCRIPT QUANTITIES DO NOT VARY, SUBSCRIPT QUANTITIES OR ENCIRCLED QUANTITIES DO VARY TO DESCRIBE COLUMNS AND/OR ROWS OF MATRICES. BROKEN BRACKETS INDICATE ROW MATRICES, CURLY BRACKETS COLUMN MATRICES, AND SQUARE BRACKETS TWO-DIMENSIONAL MATRICES.) THUS, LOWERING SUPERSCRIPTS OR RAISING SUBSCRIPTS SIMPLY IMPLIES NOTATIONAL REORDERING. HOWEVER, PHYSICAL REORDERING ON THE COMPUTER IS NOT REQUIRED, SINCE THE IMPLIED REORDERING IS ACHIEVED BY COMPUTER SUBSCRIPTING.

2. THE NOTATION OF THE TEXT IS PRESERVED, IN THAT W INDICATES NEAR-FIELD DATA, w INDICATES FAR-FIELD DATA, AND n, m, m' CORRESPOND TO THE USAGE GIVEN IN THE TEXT. HOWEVER, THE SUPERSCRIPTS A AND t ARE DROPPED (BOTH μ AND t ARE REDUNDANT), AND μ' IS INTRODUCED TO DISTINGUISH THE FAR-FIELD μ FROM THE NEAR-FIELD μ.

3. THE QUANTITY $f^{nmm'1}$ IS EXPLICITLY GIVEN AS IT DIFFERS FROM THE DEFINITION OF APPENDIX I. HERE, THE f's ARE PURE-REAL NUMBERS. ALSO, ONLY THE f's CORRESPONDING TO POSITIVE SUPERSCRIPT QUANTITIES ARE STORED, AS A SIMPLE SIGN CHANGE GIVES THE QUANTITIES CORRESPONDING TO NEGATIVE SUPERSCRIPTS. THE ELEMENTS OF THE Π ARRAY ARE COMPUTED AS THEY ARE NEEDED.

4. DISK STORAGE IS INDICATED FOR ELECTRICALLY LARGE ANTENNAS WHICH REQUIRE MANY MEASUREMENT POINTS. ON SMALLER ANTENNAS, OR WHEN MEASUREMENT ACCURACY IS NOT CRUCIAL, TAPE STORAGE AND/OR STORAGE IN CENTRAL MEMORY ALONE MAY BE UTILIZED.
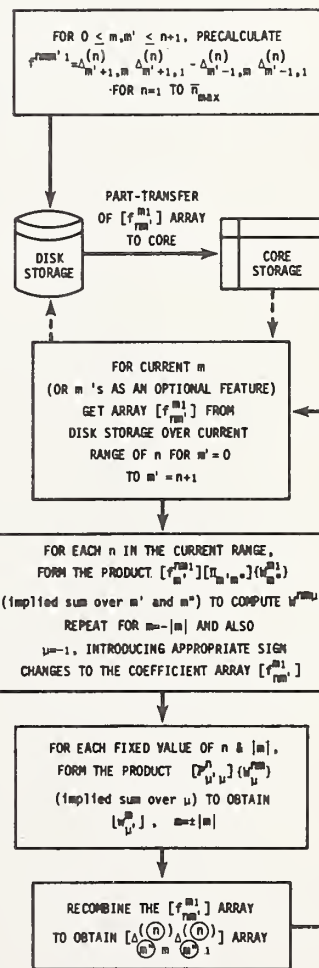
Table 1. Symmetry Properties of Scanning Systems.

	Circle (Fourier Series)	Line (Fourier Transform)	Plane	Circular Cylinder	Sphere
R	$\phi_0(r_0, z_0)$	$x_0(y_0, z_0)$	$x_0, y_0, (z_0)$	$\phi_0, z_0, (r_0)$	$\phi_0, \theta_0, \chi_0, (r_0 = A)$
n	n	k_x	k_x, k_y	n, k_z	n
m	--	--	--	--	m
$D^{(n)}_{m\mu}(R)$	$e^{+in\phi_0}$	$e^{+ik_x x_0}$	$e^{+i(k_x x_0 + k_y y_0)}$	$e^{+i(n\phi_0 + k_z z_0)}$	$e^{im\phi_0} d^{(n)}_{m\mu}(\theta_0) e^{iu\chi_0}$
scalar $f^{(n)}_m(P)$	$e^{-in\phi}$	$e^{-ik_x x}$	$e^{-i(k_x x + k_y y)}$	$e^{-i(n\phi + k_z z)}$	$e^{im\phi} P_n^m(\cos\theta)$
$\rho(R)$	$1/(2\pi)^{1/2}$	$1/(2\pi)^{1/2}$	$1/2\pi$	$1/2\pi$	$(\sin\theta_0)/8\pi^2$
Group	C_∞	T_1	$T_2 = T_1 \times T_1$	$C_\infty \times T_1$	$O^+(3)$

Computation of the Multiplying Matrices

The d's are given by

$$d_{m\mu}^{(n)}(\theta_o) = \Delta_{0m}^{(n)}\Delta_{0\mu}^{(n)}\kappa(0) + 2\sum_{m'>o}\Delta_{m'm}^{(n)}\Delta_{m'\mu}^{(n)}\kappa(m'\theta_o) \quad (I.1)$$

where $\Delta_{m\mu}^{(n)} \equiv d_{m\mu}^{(n)}(\pi/2)$ and

$$\kappa(x) = \cos x \quad \text{if} \quad m - \mu = 0 + 4k$$
$$= \sin x \quad \text{if} \quad m - \mu = 1 + 4k$$
$$= -\cos x \quad \text{if} \quad m - \mu = 2 + 4k$$
$$= -\sin x \quad \text{if} \quad m - \mu = 3 + 4k$$

where k is any integer [Edmonds (4.5.2)]. Equation (I.1) is a Fourier decomposition and is easily converted from the sin-cos to the exponential representation. For fixed m and μ, one may then write

$$\{d_{m\mu}^{(n)}(\theta_0)\} = [\delta_{nm'}^{m\mu}]\{e^{im'\theta_0}\}, \quad (I.2)$$

where the left hand side is a column matrix with the row index $n \geq |m|, |\mu|$; the last factor is a column matrix with the row index m'; and $[\delta_{nm'}^{m\mu}]$ is a rectangular matrix with row and column indices n and m' respectively. The $\sin\theta_o$ factor is easily introduced, i.e.,

$$\{d_{m\mu}^{(n)}(\theta_0)\sin\theta_0\} = [f_{nm'}^{m\mu}]\{e^{im'\theta_0}\}, \quad (I.3)$$

where

$$[f_{nm'}^{m\mu}] = \frac{[\delta_{n,m'-1}^{m\mu}] - [\delta_{n,m'+1}^{m\mu}]}{2i}. \quad (I.4)$$

Thus, the problem is reduced to computing the Δ's.

The Δ's, like all d's, are real (Edmonds, p. 59]. The array of Δ's, which are numbers, may be considered to form a pyramid as shown in figure 5, where $n = 0$ to ∞ is the vertical

distance down from the apex, and m' and m are coordinates orthogonal to both each other and the axis of the pyramid. Both m' and m assume values from -n to +n; and n, m', and m assume only integer values. From equation (I.1), negative values of m' are unneeded (or in the exponential representation can easily be obtained from the properties of the sine and cosine). This combined with symmetry relations among the d's [Edmonds, pp. 59-60] permits one to confine computations for each n (horizontal plane) to the triangle defined by m' $\geq$ 0, m $\geq$ 0, m' $\geq$ m, the remaining Δ's being obtainable by multiplying by an appropriate integer power of -1.

The Δ's are easily obtained on the vertical m = 0 and m' = 0 planes and also on the exterior faces, namely

$$\Delta_{m'0}^{(n)} = 0 \text{ for } n + m' \text{ odd}$$

$$= \frac{2^{m'}}{\sqrt{\pi}} (-1)^{\frac{n+m'}{2}} \frac{\Gamma(\frac{n+m'+1}{2})}{(\frac{n-m'}{2})!} \sqrt{\frac{(n-m')!}{(n+m')!}} \text{ for } n + m' \text{ even} \quad (I.5)$$

[See Edmonds (4.1.24) and NBS Handbook of Mathematical Functions (8.6.1)] and

$$\Delta_{nm}^{(n)} = \frac{1}{2^n} \sqrt{\frac{(2n)!}{(n+m)! \ (n-m)!}} \quad (I.6)$$

[see Edmonds (4.1.27) and (4.2.6)]. Computation of the remaining values of the Δ's within the triangle is expected to be most efficient by means of recursion formulas. The coefficients of the sines or cosines in equation (I.1) are given by products of corresponding Δ's on two planes with m in figure 5 equal to m and μ respectively.

Translational Transformation of the Probe Pattern Coefficients

To carry out the translational transformation of the probe pattern coefficients (15), we require expressions for the $c_{\sigma\mu\nu}^{sn}$'s, i.e., expressions for the coefficients in the expansions of the probe modes in terms of the test antenna modes. Depending upon whether the probe receives or transmits, the probe modes in the probe coordinate system involve spherical Hankel functions of the first or second kind. We require an expression valid inside the scanning sphere, i.e., for $r < r_0 = A$. For simplicity, the translation is assumed to be along the z axis, the effect of subsequent rotation being given by (16). The forms given by Bruning and Lo [1971, (22), (23), p. 390] are most convenient. Thus,

$$\underline{M}_{\mu\nu}^{(j)'} = \sum_{n=[\mu]}^{\infty} A_{\mu n}^{\mu\nu} \, \underline{M}_{\mu n}^{(1)} + B_{\mu n}^{\mu\nu} \, \underline{N}_{\mu n}^{(1)} \tag{II.1}$$

and

$$\underline{N}_{\mu\nu}^{(j)'} = \sum_{n=[\mu]}^{\infty} A_{\mu n}^{\mu\nu} \, \underline{N}_{\mu n}^{(1)} + B_{\mu n}^{\mu\nu} \, \underline{M}_{\mu n}^{(1)} \tag{II.2}$$

where

$$A_{\mu n}^{\mu\nu} = (-1)^{\mu} \, i^{n-\nu} \, \frac{2n+1}{2n(n+1)} \sum_{p} i^{-p} [n(n+1)+\nu(\nu+1)-p(p+1)]$$
$$\cdot \, a(\mu,\nu,-\mu,n,p) \, h_p^{(j)}(kA), \tag{II.3}$$

$$B_{\mu n}^{\mu\nu} = (-1)^{\mu} \, i^{n-\nu} \, \frac{2n+1}{2n(n+1)} \sum_{p} i^{-p} (-2i\mu kA) \, a(\mu,\nu,-\mu,n,p) \, h_p^{(j)}(kA), \tag{II.4}$$

$$a(\mu,\nu,-\mu,n,p) = (2p+1)[(\nu+\mu)!(n-\mu)!/(\nu-\mu)!(n+\mu)!]^{1/2}$$
$$\cdot \begin{pmatrix} \nu & n & p \\ 0 & 0 & 0 \end{pmatrix} \begin{pmatrix} \nu & n & p \\ \mu & -\mu & 0 \end{pmatrix}, \tag{II.5}$$

and the last two factors are Wigner 3-j coefficients [Edmonds, pp. 45-52]. Here the primed modes on the left hand sides of (II.1) and (II.2) are functions of the probe coordinates r', θ', and ϕ' and the unprimed modes on the right are functions of the test antenna coordinates r, θ, and ϕ. The normalizations assume that $f_m^{(n)}$ of (6') and (6") is taken, e.g., as $z_n(kr) P_n^m(\cos \theta) e^{im\phi}$ where z_n is a spherical Bessel function. The (j) on the left hand sides of (II.1) and (II.2) and the right hand sides of (II.3) and

(II.4) indicates the type of Hankel function, while the (1) on the right hand sides of (II.1) and (II.2) indicates spherical Bessel functions of the first kind (j_n's). The summation index $[\mu]$ in the first two equations indicates the larger of unity and the absolute value of μ. Although the upper limit is infinite, the A's and B's are needed only for the n's for which the test antenna pattern coefficients (Q^{smn}'s of (16)) are significant. The sums over p in the second two equations are from $|n-\nu|$ to $n+\nu$ for p values such that $J = n+\nu+p$ is even. Hence, for small probes, only a small number of p values are required, ν being unity for an ideal dipole.

To avoid unnecessary computations in the transformations proper, special normalizations are used; for brevity, we confine our attention to the $\mu = \pm 1$ case. We define

$$h_p^{(j)}(kA) = (2p+1)\, i^{-p}\, h_p^{(j)}(kA), \tag{II.6}$$

$$\underline{M}_{\mu\nu}^{(j)\,\prime} = i^{\nu}\, \underline{M}_{\mu\nu}^{(j)\,\prime}, \tag{II.7}$$

$$\underline{M}_{\mu n}^{(1)} = \frac{(2n+1)}{4n^2(n+1)^2}\, i^n\, \underline{M}_{\mu n}^{(1)}, \tag{II.8}$$

and similarly for the $\underline{N}$'s. We then obtain

$$\underline{M}_{\mu\nu}^{\prime\,(j)} = \sum_{n=[\mu]}^{\infty} A_{\mu n}^{\mu\nu}\, \underline{M}_{\mu n}^{(1)} + B_{\mu n}^{\mu\nu}\, \underline{N}_{\mu n}^{(1)} \tag{II.9}$$

and

$$\underline{N}_{\mu\nu}^{\prime\,(j)} = \sum_{n=[\mu]}^{\infty} A_{\mu n}^{\mu\nu}\, \underline{N}_{\mu n}^{(1)} + B_{\mu n}^{\mu\nu}\, \underline{M}_{\mu n}^{(1)}, \tag{II.10}$$

where

$$A_{-1n}^{-1\nu} = A_{1n}^{1\nu} = \sum_{p} [n(n+1)+\nu(\nu+1)-p(p+1)]^2$$
$$\cdot \frac{\lceil J-2n\rceil \lceil J-2\nu\rceil \lceil J-2p\rceil}{(J+1)\, \lceil J\rceil}\, h_p^{(j)}(kA), \tag{II.11}$$

$$-B_{-1n}^{-1\nu} = B_{1n}^{1\nu} = -2ikA \sum_{p} [n(n+1)+\nu(\nu+1)-p(p+1)]^1$$
$$\cdot \frac{\lceil J-2n\rceil \lceil J-2\nu\rceil \lceil J-2p\rceil}{(J+1)\, \lceil J\rceil}\, h_p^{(j)}(kA), \tag{II.12}$$

⌈J⌉ equals the binomial coefficient $\binom{J}{J/2}$, and the summation constraints are unchanged.

Since $j_n = h_n^{(1)} + h_n^{(2)}$, the preceding expressions also express the incoming modes in the test antenna coordinate system arising from a transmitting probe or vice versa. Hence,

$$c_{\sigma\mu\nu}^{sn}(A) = A_{\mu n}^{\mu\nu} \delta_{s\sigma} + B_{\mu n}^{\mu\nu} \delta_{s,\sigma+1} \qquad (II.13)$$

where $\delta_{s,\sigma+1}$ is unity if the probe and test antenna modes are of different TE,TM types, otherwise zero. Finally, we compute the P's as

$$P^{s\mu nAt} = (-1)^\mu [(n+\mu)!/(n-\mu)!]^{1/2} \, p^{s\mu nAt} \qquad (II.14)$$

so that they are the coefficients of partner function modes and thus equation (16) is valid without additional normalization factors.

REFERENCES

Bennett, C.A., and N.L. Franklin, Statistical Analysis in Chemistry and the Chemical Industry. (John Wiley and Sons, New York, 1954).

Brand, Louis, Vector and Tensor Analysis. (John Wiley and Sons, New York, 1947).

Bruning, J.H., and Y.T. Lo, Multiple Scattering by Spheres, Technical Report No. 69-5 (Antenna Laboratory, Department of Electrical Engineering, University of Illinois, Urbana, Illinois, 1969).

Bruning, J.H., and Y.T. Lo, "Multiple Scattering of EM Waves by Spheres ...," IEEE Trans. Antennas Propagat., Vol. AP-19, pp. 378-390, (May 1971).

Cruzan, O.R., "Translational Addition Theorems for Spherical Vector Wave Functions," J. Quart. Appl. Math., Vol. 20, pp. 33-40 (1962).

Edmonds, A.R., Angular Momentum in Quantum Mechanics (Princeton University Press, Princeton, 1957).

Erdélyi, A., Higher Transcendental Functions, Vol. II (McGraw-Hill Book Co., Inc., New York, 1953).

Haig, F.R., T.F. Jordan, and A.J. Macfarlane, Group Theory and Modern Analysis (University of Rochester, Rochester, N.Y., 1963).

Hamermesh, M., Group Theory and its Application to Physical Problems (Addison-Wesley Publ. Co., Reading, Mass., 1962).

James, J.R., and L.W. Longdon, "Prediction of Arbitrary Electromagnetic Fields from Measured Data," Alta Frequenza, vol. 38, Numero Speciale, pp. 286-290, (May 1969).

Jensen, F., Electromagnetic Near-Field Far-Field Correlations LD-15 (Technical University of Denmark, Lyngby, 1970).

Jensen, F., "On Probe Compensation for Near-Field Measurements on a Sphere," forthcoming paper in Archiv für Electronik und Übertragungstechnik (Electronics and Communications), (1975).

Kerns, D.M., "Analysis of Symmetrical Waveguide Junctions," J. Res. NBS, vol. 46, pp. 267-282, (1951).

Kerns, D.M., and E.S. Dayhoff, "Theory of Diffraction in Microwave Interferometry," J. Res. NBS, vol. 64B, pp. 1-13, (1960).

Kerns, D.M., "Correction of Near-Field Antenna Measurements made with an Arbitrary but Known Measuring Antenna," Electron. Lett., vol. 6, pp. 346-347, (1970).

Kerns, D.M., Matrix Description of Waveguide N-Ports, unpublished NBS Report, (1971).

Leach, W.M., Jr., and D.M. Paris, "Probe-compensated Near-Field Measurements on a Cylinder," IEEE Trans. Antennas Propagat., vol. AP-21, pp. 435-445, (July 1973).

Miller, W., Jr., Lie Theory and Special Functions (Academic Press, New York, 1968).

Morse, P.M., and H. Feshbach, Methods of Theoretical Physics (McGraw-Hill, New York, 1953).

Newell, A.C., R.C. Baird, and P.F. Wacker, "Accurate Measurement of Antenna Gain and Polarization at Reduced Distances by an Extrapolation Technique," IEEE Trans. Antennas Propagat., vol. AP-21, pp. 418-431, (July 1973).

Newell, A.C., and M.L. Crawford, Planar Near-Field Measurements on High Performance Array Antennas, NBSIR 74-380 (National Bureau of Standards, Boulder, Colo., 1974).

Pontrjagin, L., Topological Groups (Princeton Univ. Press, Princeton, 1946).

Riesz, F. and B. Sz.-Nagy, Functional Analysis (F. Ungar Publ. Co., New York, 1955).

Rodrigue, G.P., E.B. Joy, and C.P. Burns, An Investigation of the Accuracy of Far-Field Radiation Patterns Determined from Near-Field Measurements (Georgia Institute of Technology, Atlanta, 1973).

Stein, S., "Addition Theorems for Spherical Wave Functions," J. Quart. Appl. Math., vol. 19, pp. 15-24, (1961).

Stratton, J.A., Electromagnetic Theory (McGraw-Hill, New York, 1941).

Wacker, P., "Near-Field Antenna Measurements Using a Spherical Scan: Efficient Data Reduction with Probe Correction," in Conference on Precision Electromagnetic Measurements, IEE Conference Publication No. 113 (IEE, London, 1974).

U.S. DEPT. OF COMM. BIBLIOGRAPHIC DATA SHEET	1. PUBLICATION OR REPORT NO. NBS-IR 75-809	2. Gov't Accession No.	3. Recipient's Accession No.

4. TITLE AND SUBTITLE Non-Planar Near-Field Measurements: Spherical Scanning	5. Publication Date June 1975
	6. Performing Organization Code

7. AUTHOR(S) Paul F. Wacker	8. Performing Organ. Report No.

9. PERFORMING ORGANIZATION NAME AND ADDRESS NATIONAL BUREAU OF STANDARDS DEPARTMENT OF COMMERCE WASHINGTON, D.C. 20234	10. Project/Task/Work Unit No. NBS 2767486, AFAL F33615-74-M-6001
	11. Contract/Grant No. AFAL F33615-74-M-6001

12. Sponsoring Organization Name and Complete Address (Street, City, State, ZIP) Air Force Avionics Laboratory (AFSC) Wright-Patterson Air Force Base, Ohio 45433	13. Type of Report & Period Covered Final, Oct., 1973- June, 1974
	14. Sponsoring Agency Code

15. SUPPLEMENTARY NOTES

Being issued both as AFAL Technical Report AFAL-TR-75-38 and as NBSIR 75-809.
Supported both by AFAL and NBS.

16. ABSTRACT (A 200-word or less factual summary of most significant information. If document includes a significant bibliography or literature survey, mention it here.) The advantages and limitations of near-field antenna measurements are compared with those of conventional far-field measurements. Further, the advantages and limitations of planar, circular cylindrical, and spherical scanning are compared.

Spherical scanning is advantageous for arrays steered well off-axis and for antennas with wide angle side lobes, but the data processing has been quite impractical except for very simple antennas and probes. A new highly efficient data processing scheme is given for spherical scanning with and without probe pattern correction. The translation-of-centers transformation of the probe pattern coefficients (required only with the probe pattern correction) is carried out once and for all for a given probe, scanning radius, and frequency. The routine computations involve Fast Fourier "Transforms" and multiplication by matrices with constant elements, matrices which are independent of the detailed nature of the probe, the radius of the scanning sphere, the points at which measurements are made, and the nature of the test antenna. The FFT's and matrix multiplications supplant matrix inversion, ordinary solution of simultaneous equations in more than two unknowns, ordinary numerical integration, and (in routine processing) ordinary evaluation of functions, even for computation of the far field. Except for the truncation of the infinite series of spherical modes, no analytical or data processing approximations are made, even in the use of the FFT.

So that readers may draw from their understanding of planar and cylindrical scanning, a unified theory of near-field data processing is given, treating planar, cylindrical, and spherical scanning as mere special cases.

17. KEY WORDS (six to twelve entries; alphabetical order; capitalize only the first letter of the first key word unless a proper name; separated by semicolons)
Antennas; arrays; coordinate transformations; data processing; group representations; measurements; near field; non-planar; patterns; scanning; spherical; symmetry.

18. AVAILABILITY ☒ Unlimited	19. SECURITY CLASS (THIS REPORT)	21. NO. OF PAGES
☐ For Official Distribution. Do Not Release to NTIS	UNCLASSIFIED X	69
☐ Order From Sup. of Doc., U.S. Government Printing Office Washington, D.C. 20402, SD Cat. No. C13	20. SECURITY CLASS (THIS PAGE)	22. Price
☒ Order From National Technical Information Service (NTIS) Springfield, Virginia 22151	UNCLASSIFIED X	$4.25